Life Cycle Stage-resolved Proteomic Analysis of the Excretome/Secretome from *Strongyloides ratti*—Identification of Stage-specific Proteases*[S]

Hanns Soblik‡, Abuelhassan Elshazly Younis‡§, Makedonka Mitreva¶‖, Bernhard Y. Renard‡‡, Marc Kirchner§§, Frank Geisinger‡, Hanno Steen§§¶¶‖‖, and Norbert W. Brattig‡¶¶‖‖**

A wide range of biomolecules, including proteins, are excreted and secreted from helminths and contribute to the parasite's successful establishment, survival, and reproduction in an adverse habitat. Excretory and secretory proteins (ESP) are active at the interface between parasite and host and comprise potential targets for intervention. The intestinal nematode *Strongyloides spp.* exhibits an exceptional developmental plasticity in its life cycle characterized by parasitic and free-living generations. We investigated ESP from infective larvae, parasitic females, and free-living stages of the rat parasite *Strongyloides ratti,* which is genetically very similar to the human pathogen, *Strongyloides stercoralis*. Proteomic analysis of ESP revealed 586 proteins, with the largest number of stage-specific ESP found in infective larvae (196), followed by parasitic females (79) and free-living stages (35). One hundred and forty proteins were identified in all studied stages, including anti-oxidative enzymes, heat shock proteins, and carbohydrate-binding proteins. The stage-selective ESP of (1) infective larvae included an astacin metalloproteinase, the L3 Nie antigen, and a fatty acid retinoid-binding protein; (2) parasitic females included a prolyl oligopeptidase (prolyl serine carboxypeptidase), small heat shock proteins, and a secreted acidic protein; (3) free-living stages included a lysozyme family member, a carbohydrate-hydrolyzing enzyme, and saponin-like protein. We verified the differential expression of selected genes encoding ESP by qRT-PCR. ELISA analysis revealed the recognition of ESP by antibodies of *S. ratti*-infected rats. A prolyl oligopeptidase was identified as abundant parasitic female-specific ESP, and the effect of pyrrolidine-based prolyl oligopeptidase inhibitors showed concentration- and time-dependent inhibitory effects on female motility. The characterization of stage-related ESP from *Strongyloides* will help to further understand the interaction of this unique intestinal nematode with its host. ***Molecular & Cellular Proteomics 10: 10.1074/mcp. M111.010157, 1–16, 2011.***

The successful establishment of nematodes in the intestinal habitat of a mammalian host and subsequent survival for an extended period of time in the adverse biotope, hinges upon the ability of the parasitic nematode to generate an array of molecules that interfere with the host's defense system endeavored to eliminate the untoward lodger (1). Excretory and secretory (E/S)[1] and some somatic products released from living and moribund helminth parasites, respectively, are initial factors, including proteases, enzyme regulators, anti-oxidative proteins, transporters, and various ligand-binding proteins (2). E/S products, active at the interface between the parasite and host are currently intensely investigated as potential targets for therapeutic intervention.

In evolutionary terms, long-lasting interaction between intestinal parasitic nematodes and mammalian hosts has led to increased adaptation and co-evolution (3). The "old friend" hypothesis assumes that the presence of certain helminths and microbes chronically colonizing the intestine stimulates the host's immunoregulatory system to tolerate these "harmless," yet foreign, organisms. It is currently hypothesized that increases in chronic inflammatory disorders, such as inflammatory bowel diseases and allergies, in developed countries

From the ‡Bernhard Nocht Institute for Tropical Medicine, 20359 Hamburg, Germany; §Zoology Department, Aswan Faculty of Science, South Valley University Aswan, Egypt; ¶The Genome Institute, Washington University School of Medicine, St. Louis, Missouri 63108; ‖Department of Genetics, Washington University School of Medicine, St. Louis, Missouri 63108; **Computational Medicine Unit, Institute for Translational Oncology and Immunolgy, University Mainz, Germany; ‡‡Research Group Bioinformatics, Robert Koch-Institute, Nordufer 20, 13353 Berlin, Germany; §§Proteomics Center at Children's Hospital Boston, and Departments of Pathology, Children's Hospital Boston and Harvard Medical School, Boston, Massachusetts 02115

⌘ *Author's Choice*—Final version full access.

Received April 1, 2011, and in revised form, September 26, 2011

Published, MCP Papers in Press, September 30, 2011, DOI 10.1074/mcp.M111.010157

[1] The abbreviations used are: E/S, excretory/secretory; ESP, excretory/secretory proteins; iL3, infective larvae; pF, parasitic female; flS, free-living stages; flF, free-living females; PSC, prolyl serine carboxypeptidase; EST, expressed sequence tag.

are partially attributable to diminished exposure to organisms that were part of mammalian evolutionary history (4).

Strongyloides generates infective, parasitic and free-living stages, making this parasite genus ideally suited for investigating E/S products and enabling the identification and characterization of proteins with pivotal relevance for its parasitic lifestyle and putative immune-modulating capability. The human pathogen *Strongyloides stercoralis* shows several fundamental differences to the other helminths: (1) In contrast to other soil-transmitted helminths, the unique life cycle of *S. stercoralis* encompasses both, a direct (asexual) and—facultatively—an indirect (sexual) development (5). Thus, in contrast to *e.g. Ascaris* and hookworm, the *Strongyloides* larvae can develop *ex vivo* into adults resulting in sexual reproduction and egg formation; infective larvae (iL3) eventually hatch from these eggs. (2) *S. stercoralis* exhibits the ability to complete its life cycle within the human host. Accordingly, larvae can develop to the iL3 within the gastrointestinal tract, traverse the intestinal mucosa, migrate through the tissues, and establish again in the small intestine (6). Such cycles of autoinfection can lead to repeated re-infection that can persist for several decades without apparent symptoms. (3) No other human parasitic nematode has been associated with such a broad spectrum of manifestations and clinical syndromes as *S. stercoralis*. Chronic infections with *S. stercoralis* are often associated with no or mild cutaneous, gastrointestinal, or pulmonary symptoms. In immune-competent hosts, the disease is generally not life-threatening. However, in immunocompromised patients, *e.g.* after treatment with immunosuppressive drugs like glucocorticoids, after co-infection with HTLV-1, or tuberculosis, in case of hematologic malignancies, or protein-caloric malnutrition syndrome, an accelerated autoinfection (hyperinfection) normally occurs, leading, in ≥87% of the cases, to life-threatening disseminated infections and death (7, 8). Recent reports have indicated the underestimation of strongyloidiasis and its hyperinfection syndrome, which is now considered an emerging global infectious disease that has migrated from developing regions to industrialized areas (9). More than 100 million people are probably infected, as the current stool diagnostic is insensitive, and as such the number of infected people was grossly underestimated (10, 11).

To investigate E/S products (ESPs) possibly relevant in the parasite-host interaction during *Strongyloides* infection, we chose the rat-infecting *S. ratti* as a model parasite, which is genetically closely related to the human parasite *S. stercoralis* (12). This model system is highly advantageous as the life cycle is short and easily maintained, giving access to infective, parasitic, and free-living stages and their respective ESPs. In this study, the E/S products from the accessible *S. ratti* stages were collected and comprehensively analyzed using liquid chromatography (LC)/MS-based proteomics strategies. Selected proteins identified in this proteomic study were characterized and studied further. The overall objective of this study was the identification and functional characterization of molecules that are potentially important for the establishment and maintenance of parasitism and the helminth-induced immunosuppression (2, 13).

EXPERIMENTAL PROCEDURES

Maintaining S. ratti Life Cycle—The *S. ratti* life cycle established in our laboratory was provided by Dr. G. Pluschke (Swiss Tropical Institute, Basel). Wistar rats were used to maintain the life cycle by serial passage, as described previously (14, 15). Approval was obtained from the Animal Protection Board of the City of Hamburg.

Preparation of Infective Larvae (iL3)—For the isolation of iL3, fecal pellets were collected on days 6–16 after subcutaneous infection of male Wistar rats with 1800–2500 iL3s. Charcoal coprocultures (12) were established and incubated at 26 °C. The culture dishes were incubated 5–7 days for the collection of newly generated iL3. For the recovery of iL3, the Baermann method was used (16). After separation of from the charcoal coproculture the larvae were extensively washed (see below).

Preparation of Free-living Stages (flS)—For the flS preparation, fecal pellets were collected at the earliest 6 days after subcutaneous infection of rats with 1800–2500 iL3s. Charcoal coprocultures were prepared and incubated at 26 °C for 24 h. Free-living females were manually isolated from other flS using a light microscope. The free-living females (flF) were isolated from other flS by careful pipeting under the light microscope.

Preparation of Parasitic Females (pF)—For the collection of pF, the rats were infected with about 2500 iL3s. On day six and seven postinfection, the rats were sacrificed, and the small intestines between the stomach and ~10 cm before the appendix were removed. The intestines were precleaned by emptying the contents through careful squeezing of the intestinal walls. Next, the intestine was opened longitudinally using scissors and cut into strips of about 8–10 cm length. The strips were washed three times by gentle shaking in three different beakers filled with 500 ml of water or PBS to remove residual debris. To separate the female nematodes from the tissue, the strips were placed directly on the sieve without the cotton in a Baermann apparatus and incubated for 3 h. After sedimentation of the females, 50 ml of the solution in the Baermann funnel were transferred into a 50-ml conical tube. After a second sedimentation of the females, they were transferred to a 1.5-ml tube and washed six times in sterile Hanks balanced salt solution (Sigma-Aldrich, Steinheim, Germany) supplemented with 100 U/ml penicillin and 100 mg/ml streptavidin (Sigma). Between the washing steps, the tube was centrifuged at 1000 rpm for 1 min. These repeated centrifugation steps at low speed resulted in a separation of pF from tissue and residual eggs, as well as first-stage larvae as confirmed by microscopy. The suspension of parasitic females was used for *in vitro* culture or for the preparation of RNA as described (17).

Preparation of Excretory and Secretory Products—Freshly harvested and extensively washed iL3, pF, or flS were carefully suspended in sterile worm culture medium under the laminar flow hood. The washing solution consisted of Hanks Balanced Salt Solution supplemented with penicillin (100 U/ml) and streptomycin (100 μg/ml). The culture medium was RPMI 1640 (Sigma-Aldrich) supplemented with penicillin and streptomycin (same concentration as washing solution) and 10 mM HEPES (Sigma-Aldrich). The incubation densities did not exceed 30,000 iL3/ml, 15,000 flS/ml and 100 pF/ml. IL3 and pF were incubated at 37 °C for 24 h and 72 h, respectively. FlS were incubated at 26 °C for 24 h. After the incubation period, vitality and sterility were checked under the microscope. An additional test for sterility was performed by placing 5 μl of each culture medium on blood agar plates and subsequently incubating the plates at 37 °C

for 24 h. Only sterile cultures were used for further experiments. All culture supernatants were supplemented with protease inhibitors (Complete protease inhibitor mixture, Roche Diagnostics, Mannheim, Germany) and concentrated about 200-fold using microspin filters with a 10 kDa molecular weight cutoff. For the inhibition of an active astacin metalloprotease, 10 mM phenanthroline solution was added to the supernatants prior to centrifugation. Biological triplicates were generated from all studied stages.

Inhibition of Protein Release—To demonstrate active protein excretion and secretion, cycloheximide or sodium azide were added to inhibit protein synthesis. The inhibitors were added immediately prior to the incubation of iL3: cycloheximide was added to final concentrations of either 50 or 70 mM, and sodium azide was added to final concentrations of either 0.5% or 1.0% (w/v). After two hours of incubation, the culture medium was removed, an equal amount of new medium was added, and the larvae were further incubated for 24 h. In parallel, equal numbers of iL3 were incubated at 4 °C, 37 °C, and 70 °C affecting the metabolic status. After treatment of the nematodes with 70 mM cycloheximide—similarly after treatment either with sodium azide, or at 4 °C and at 70 °C—all proteins, except those proximal to the 16 kDa molecular weight marker, were absent in a silver-stained SDS-PAGE gel. In addition, no metalloprotease activity was detected (see below), confirming the notion of active biosynthesis and secretion of the identified nematode proteins (data not shown).

Protease Activity Assay—To determine whether the excretory and secretory (E/S) products show proteolytic activity, substrate gel electrophoresis was performed (18, 19). Briefly, 1% gelatin was added as a substrate to the acrylamide solution before preparing the gel. The E/S products were separated under nonreducing conditions. Because SDS inhibits the activity of enzymes, the gels were washed three times in Triton X-100 for 20 min, three times in distilled water for 5 min and finally covered with renaturation buffer (Tris-HCl, 50 mM; NaCl, 100 mM; pH 7.5). After overnight staining in Coomassie blue, the bands containing active proteases appear colorless against a blue background.

One-dimensional Electrophoresis and Tryptic Digestion of E/S Proteins (ESP)—All samples were reduced by adding 10 mM dithiotreitol and incubating at 56 °C for 45 min. For alkylation, 55 mM iodoacetamide was added, and the samples were incubated 30 min at room temperature in the dark. Subsequently, NuPAGE® LDS 4 × sample buffer (Invitrogen, Darmstadt, Germany) was added, and the samples were loaded on 12% NuPAGE® Novex® SDS-PAGE gels. After electrophoresis, gels were stained with SimplyBlue (Invitrogen) protein stain. Entire gel lanes were cut into 30–40 pieces using a disposable scalpel. Prior to tryptic digestion, gel pieces were washed 5 min in 0.1 M ammonium bicarbonate, destained in 50 mM ammonium bicarbonate buffer containing 1/3 acetonitrile for 60 min, and finally dehydrated in 100% acetonitrile.

For in-gel tryptic digestion, the gel pieces were hydrated for 45 min in sequencing grade trypsin solution (12.5 ng/μl; Promega) on ice. The remaining trypsin solution was removed, gel pieces were covered with 50 mM ammonium bicarbonate and incubated overnight at 37 °C. After overnight incubation, the supernatants containing the majority of the tryptic peptides were transferred into new 1.5-ml Eppendorf tubes. The gel pieces were washed in ammonium bicarbonate containing 1/3 acetonitrile, and the washing buffer was pooled with the respective supernatant. Remaining peptides were extracted with 100% acetonitrile, which was added to the pooled supernatant and washing solution.

Mass Spectrometric Analysis—Peptides derived from in-gel digested proteins were analyzed by online microscale capillary reversed-phase HPLC hyphenated to a linear ion trap mass spectrometer (LTQ, Thermo Scientific). Samples were loaded onto an in-house packed 100 mm i.d. × 15 cm C18 column (Magic C18, 5 mm, 200 Å, Michrom Bioresource, Auburn, CA) and separated at ~ 500 nl/min with 34 min linear gradients from 6–32% acetonitrile in 0.4% formic acid. The instrument was operated in data dependent acquisition mode with a dynamic exclusion of 45 s: after each survey spectrum (*m/z* 350 to 1400), the six most intense ions per cycle were selected for fragmentation by collision-induced dissociation.

Protein Identification and Sequence Analysis—The .raw files were converted into .mgf files using in-house written scripts (20, 21). For each fragment ion spectrum, only the 200 most intense fragment ions were exported into the mgf file. The mass spectrometry data were searched against a custom database comprising translated expressed sequence tags (EST) contig sequences and protein sequences from *S. ratti* and *S. stercoralis* (22) available at www.nematode.net (23), and other protein sequences from *Brugia malayi* and *Caenorhabditis elegans* (supplemental Table S1), totalling 39,318 sequences. Searches were performed using ProteinPilot™ (version 2.0.1; AB/Sciex) using the following search parameters: Sample Type, Identification; Cys Alkylation, Iodoacetamide; Digestion, Trypsin; Instrument, LTQ; Special Factors, Gel-based ID; ID Focus, Amino acid substitutions; Search Effort, Thorough. Proteins were identified based on a minimum unused protein score (UPS) of 4.00 equal to two or more unique peptides of 99% confidence. Protein inference is based on the ProGroup algorithm integrated into ProteinPilot. Using a mixed model approach to estimate the confidence of the protein identifications (21), we calculated an overall protein false discovery rate of 2.17% for the cutoff score applied to the protein identifications.

EST contig sequences were subjected to Basic Local Alignment Search Tool (BLAST) searches with NCBI protein BLAST algorithm (blastp) using the default setting against the nonredundant database without any species restrictions. The top hits, irrespective of E-value and/or species are listed in the tables. The resulting sequences were screened for signal peptide for secretion using SignalP 3.0 (24).

Supernatant Versus Extract Protein Abundance Correlations—We used a rank-order correlation analysis in order to robustly determine the degree of similarity between relative protein abundances in the supernatant and the extract. Briefly, we (1) extracted total protein abundance measurements (spectral counting and/or total score) for all proteins observed in the supernatant as well as in the extract; (2) determined the rank of each measurement, accounting for ties where necessary; and (3) calculated the Spearman rank correlation coefficient between supernatant and extract ranks. All calculations were performed in Microsoft Excel.

Analysis of Relative Gene Expression Levels by qRT-PCR—Real-time PCR was used to measure relative levels of expression of selected genes from iL3, pF, and free-living females (flF). Ten genes were selected from the 25 highest scoring ESPs, including two ESP from iL3, five ESP from pF and three ESP from flS (Table I) and in addition two proteins found in all studied stages (see supplemental Table S2) were selected for quantitative RT-PCR analysis. For constitutive protein control, the *S. ratti* glyceraldehyde-3-phosphate dehydrogenase (*Sr-gapdh*) and *Sr-actin* were included. Total RNA was extracted, quantified, purified, and reverse transcribed separately from two different biological samples of the developmental stages (iL3, pF and flF) after 7 days of infection as described (17). An aliquot of ~5 μg purified parasite RNA with confirmed quality *via* the detection of discrete 18 S and 28 S ribosomal RNA bands on ethidium bromide-stained gel was used to confirm equally in each developmental stage. The forward and reverse primers for the *Sr*-genes were designed with primer3plus (http://www.bioinformatics.nl/cgi-bin/primer3plus/primer3plus.cgi) such that each amplicon was around 150 bp. Primers were analyzed using the Oligonucleotide Properties Calculator (http://www.basic.northwestern.edu/biotools/oligocalc.html) to avoid secondary structures such as hairpins, loops, and

TABLE I
Genes and dedicated primers applied in the qRT-PCR

Gene	Cluster	Accession N°	Stage: Protein list (N°)	Forward primer	Reverse primer	Amplicon (bp)
Sr-astacin	SR11111	AAK55800	iL3:Table II A (5)	TTGATACAGGAGTA AATGAAACTACAG	CCAACATATGA TCGACAACCA	145
Sr-ZK1073.1	SR02886	XP_001899587	iL3: Table II A (2)	TTGTAGATTTGC CATTGCTCATCC	TCCCAAGCACTTT GAGTCATAATTC	150
Sr-PSC-1	SR01641	NP_971802	pF: Table II B (7)	TGATGGTAAATTA GATCGTGATGAGA	CATAATGTTGGATA ATCTCTTCTGGTGA	150
Sr-calumenin	SR00564	NP_001024806	pF: Table II B (8)	TGATGGTAAATTA GATCGTGATGAGA	CATAATGTTGGATA ATCTCTTCTGGTGA	149
Sr-chitin binding protein	SR04455	XP_001664881	pF: Table II B (10)	ATGATACTAAGAA ACCTTTTACTCAAG	GTATTGACCATCA GGACATGAACTG	152
Sr-trypsin inhibitor-like protein	SR02054	XP_001866937	pF: Table II B (11)	CTTCCAACTGTC CAACAACTCAAA	CAGAAATACACTC ACATTTTGGTGGT	150
Sr-phosphoribosyl-transferase	SR02118	XP_001895434	pF: Table II B (22)	GGAACTGATTCA ACTGGACATTTAC	TTGATGCTCCATT GTCATTAACTGT	151
Sr-MFP2B	SR00863	AAP94889	fIS: Table II C (2)	ATGCCAAATCTTAA ACCAGCTAAAGAAG	AGCTCTTCCATGA ATTGGTTTTCCAT	150
Sr-CBG22129; Y51F10.7	SR02091	XP_001667627	fIS: Table II C (4)	TCTCAAGGATTAG TACTTCCAAAAAC	TCCTTTATCATCAG TAATTTGAGCTTT	150
Sr-lysozyme family	SR00671	NP_502193	fIS: Table II C (5)	TTACTGGATTCG ATGCCATTGGAA	ACCAGCTTTCACA GCATTTTTTATATT	155
Sr-galectin-2	SR00627	AAF63405	All stages: Suppl. Table II (66)	CAAGCTGGAGAA TGGGGTAATGAGG	ATCACAACGATGA GCAAAAGTGCAG	150
Sr-galectin-1	SS00840	AAD39095	All stages: Suppl. Table II (64)	GGAATGCCTGAAA AAAAAGGTAAACG	CTCTCTCTTCATT ACCCCATTCACC	150
Sr-GAPDH	SR00526	NP_508534	-	GTACCACTAAC TGTTTAGCTCC	GCACCTCTTC CATCTCTCC	154

complementarity. The RT-PCR products were evaluated by agarose gel electrophoresis.

ABI PRISM® 7000 SDS/Relative quantification system (Applied Biosystems, Foster City, CA, USA) was used to quantify the relative expression of the selected genes. *Sr*-GAPDH, which showed a constant and equal expression within the three stages, was included as a housekeeping gene for normalization purposes. PCR was performed using the qPCR Core kit for SYBR® Green I (Eurogentec S.A.) following the manufacturer's protocol. Serial cDNA dilution curves were produced to calculate the amplification efficiency for all genes (25).

For measurement of gene expression levels, each sample was tested in triplicate, using positive controls, template-free controls, negative reverse transcription control and the resulting threshold cycle value Cts recorded. The specificity and identity of individual amplicons were verified by melting curve analysis. Relative transcriptional differences were calculated from normalized values following the protocol described by Livak and Schmittgen (26). The data were expressed as the relative quantity of transcripts using the gene-specific transcription levels at the free-living females stage as baseline (value = 1). All of the samples were normalized to the expression levels of the constantly and equally expressed gene *Sr*-GAPDH.

Identification of the Full-length Gene Sequence of a Prolyl Oligopeptidase (Prolyl Serine Carboxypeptidase, Sr-PSC)—To obtain the 3′-cDNA end, 3′-Rapid Amplification of cDNA Ends (RACE) was performed using the GeneRace Kit (Invitrogen). The 3′-RACE method generates full-length cDNA by utilizing 3′-oligo-dT-containing primer complementary to the poly(A) tail of mRNA at the first strand cDNA synthesis. RACE fragments were then amplified by PCR using Taq polymerase, the gene-specific forward primer PSC f (GGAAAT TTA-ATGGAAATGAAACATGGT) and the oligo dT-T7II (GAGAGAGGATC-CAAGTACTAATACGACTCACTATAGG) as reverse primer. 5′ RACE was performed according to the manufacturer's protocol using the gene-specific primer PSC r (ATTGGAATCATTGTACCATCTTT). The full-length sequence was obtained by comparing the cloned (pGEM-T Easy vector, Promega) and sequenced (AGOWA-Germany) fragments. Primers including the 3′- and the 5′-ends were designed, and the full length of the *Sr*-PSC-1 cDNA was captured by PCR. The result was confirmed by sequencing using the M13 forward-, the M13 reverse- and gene-specific primers on the fragment that has previously cloned into the pGEM-T Easy vector.

Immune Recognition by ELISA and Immunoblotting with Rat Sera—Sera from 10 rats taken before and 32 days after infection with *S. ratti* iL3 were analyzed by ELISA (27) for IgG antibodies reactive against *S. ratti* proteins in the E/S products from iL3, pF and fIS. Polystyrene microtiter plates (Maxi-Sorb, Nunc) were coated with *Strongyloides* protein samples at a concentration of about 200 ng/well in carbonate buffer (pH 9.6), sealed with Saran wrap and incubated overnight at 4 °C. After removal of unbound protein and washing three times with PBS/0.05% (v/v) Tween 20, the plate was blocked with 5% (w/v) bovine serum albumin in PBS for one hour at 37 °C. Different dilutions (1:100 to 1:500) of rat sera were prepared in PBS/0.5% bovine serum albumin, added to the wells and incubated at 37 °C for one hour. Nonspecifically bound proteins were removed, and the wells were washed three times with Tris-buffered saline in 0.05% Tween 20. For detection of bound rat IgG, peroxidase-conjugated anti-rat IgG antibody was applied to a final concentration of 1:5000. Tetramethylbenzidine was used as peroxidase substrate. Data are expressed as end point titers derived from titration curves (1:100 to 1:500) (27). In addition, sera from 10 humans living in areas in West Africa endemic for *Strongyloides stercoralis* infection (28) and from two healthy Eu-

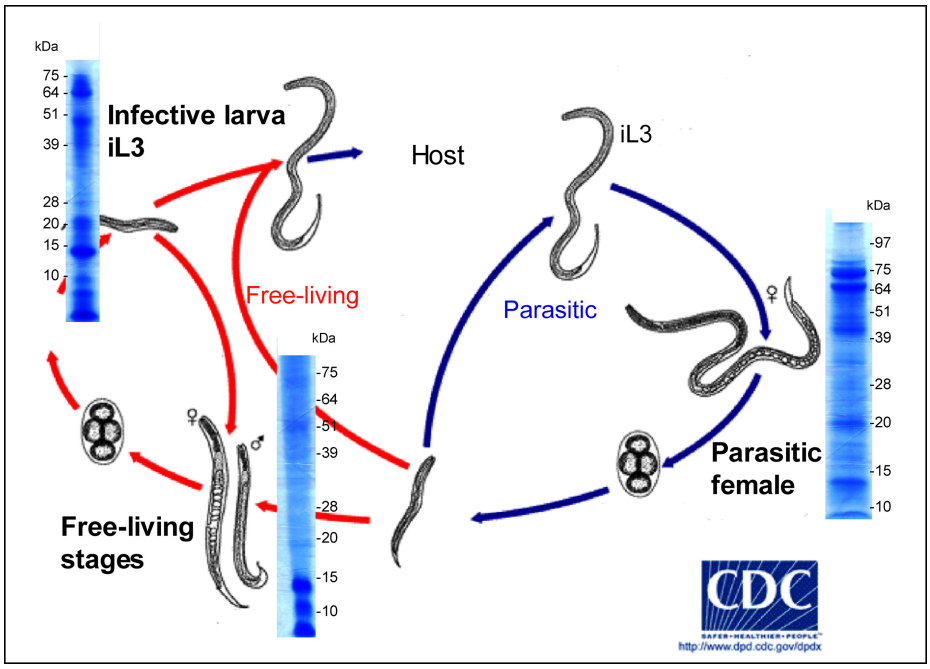

FIG. 1. **One-dimensional SDS-PAGE of E/S proteins from infective larvae, parasitic females and free-living stages showing after Coomassie stain characteristic protein band patterns of the respective stages.** The lanes are assigned to the respective stages in the life cycle (CDC, www.dpd.cdc.gov/dpdx/HTML/Strongyloidiasis.htm).

ropeans were tested for IgG recognition of *Strongyloides* proteins applying peroxidase-conjugated anti-human IgG antibody (CalBiochem, San Diego, CA). Collecting blood samples for research purpose was approved by the Ethics Commission of the Medical Board, Hamburg and by ethic committees and medical authorities in the respective countries.

Inhibition Tests for Prolyl Oligopeptidase Activity—For inhibition experiments, 0.5 M prolyl oligopeptidase inhibitor stock solutions of following compounds were applied: (1A) isophthalic acid 2(S)-(cyclopentanecarbonyl) pyrrolidine-L-prolyl-2(S)-cyanopyrrolidine amide; (1B) isophthalic acid 2(S)-(cyclopentanecarbonyl) pyrrolidine-L-prolyl-2(S)-(hydroxyacetyl)-pyrrolidine amide; (2A) 4-phenylbutanoyl-L-prolyl-pyrrolidine; and (2B) 4-phenylbutanoyl-L-prolyl-2(S)-cyanopyrrolidine (supplemental Fig. S1) (29). The compounds were dissolved in PBS and sterile filtered. The stock solutions were added directly before the incubation of pF at seven different final concentrations between 1–10 mM. The cultures were incubated at 36 °C, and the motility of the exposed females was monitored at different time points under the microscope.

Statistical Analysis—Statistical differences between the test groups of sera investigated for IgG recognition were analyzed by the Mann-Whitney *U* test. Statistical significance was considered for $p < 0.05$.

RESULTS

Proteomic Analysis of S. ratti ESP—Comparison of ESP Pattern from Different Life Cycle Stages of *S. ratti*—Active biosynthesis and excretion/secretion were confirmed under our experimental conditions by incubating the worm cultures with cycloheximide and/or sodium azide. Subsequently, we prepared life cycle stage-specific ESP samples from the following *S. ratti* life cycle stages: iL3, pF, and fIS. Each sample type was analyzed in three biological replicates, and proteins were considered to be present when discovered in one of the replicates. SDS gel electrophoretic analysis revealed protein mixtures of different complexities based on the differing banding patterns in the various ESP. The majority of the ESPs

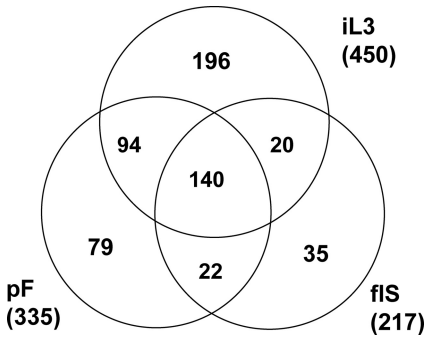

FIG. 2. **Venn diagram showing the distribution of the identified *S. ratti* E/S proteins of the studied developmental stages: iL3, pF and fIS.** The numbers in brackets show the quantities of the proteins in each stage(s) total.

from iL3 appeared to be bimodally distributed between 10–30 kDa and 40–100 kDa, whereas ESPs in the pF sample were predominantly observed at 40–100 kDa. The ESPs from the fIS sample were mainly of low-molecular weight between 10 and 15 kDa with an extensive smearing above 40 kDa (Fig. 1). The pattern of protein bands differed strongly between ESPs and somatic extracts of the stages (supplemental Fig. S2).

A total of 586 *S. ratti* proteins were identified in the ESP, 450 proteins in ESP from iL3, 335 in pF, and 217 in fIS. Approximately a quarter of the identified proteins were found in all the samples from the studied life-cycle stages, *i.e.* in iL3, pF, and in fIS (140 proteins, 23.8%, Fig. 2). Proteins abundantly observed in all three investigated developmental stages were heat-shock proteins, galectins, enzymes, fatty acid binding protein, as well as distinct structural proteins (supplemental Table S2).

The fraction of stage-specific proteins varied significantly: 33.4% (196 proteins) of the identified ESPs were found exclusively in the iL3 stage, compared with 13.5% (79 proteins) found in only in pF ESP and only 6.0% (35 proteins) in fIS. The majority of ESPs, which were observed in two studied stages, occurred in iL3 and pF (16.0%) in comparison to 3.4% and 3.8% found in fIS as well as in iL3 or in fIS and pF, respectively.

To further confirm active biosynthesis and excretion/secretion, and to exclude the possibility of accidental worm lysis resulting in the presence of cytoplasmic proteins in the supernatant, we also analyzed the proteomes of worm extracts prepared from the corresponding life cycle stages. A rank-order correlation of the identified ESP and extract protein resulted in Spearman rank correlation coefficients between 0.13 and 0.2, indicating little to no rank-order correlation, thus providing evidence in support of excretion/secretion and against worm lysis.

Identification of Stage-specific Proteins-ESP Specific for S. ratti iL3—In total, 196 proteins were identified as iL3-specific (supplemental Table S 3). Of these, 170 proteins were identified as present in either a *S. ratti* or *S. stercoralis* EST cluster. It is expected that many more proteins would have been identified if the *Strongyloides* databases had been more complete. This notion was underscored by the fact that 26 (~13%) additional proteins were identified, which were assigned to proteins from *Onchocerca volvulus* (1), *Trichuris trichiura* (1), *B. malayi* (1), *Haemonchus contortus* (1), or *C. elegans* (22) because the sequences of the respective *Strongyloides* orthologs were missing in the database. The 25 highest-scoring (based on ProteinPilot's "unused " score) iL3-specific proteins are listed in Table IIA. GO annotation of these iL3 specific ESPs assigns these proteins to a wide range of functional categories, including protein digestion and folding ($n = 7$), fatty-acid binding ($n = 2$), carbohydrate metabolism ($n = 8$), and cytosol energy metabolism ($n = 14$).

Several nominally cytosolic proteins were identified among the 25 highest-scoring iL3-specific ESPs, including thiosulfate sulfuryltransferase (SR01803), short chain reductase/dehydrogenase (SR03119), and propionyl coenzyme A carboxylase (SR00383). The above mentioned control experiments, however, convinced us that these nominally cytosolic proteins are indeed *bona fide* ESPs. Other identified proteins include the nematode-specific transthyretin-like protein family member with a suggested role in the nervous system (30).

Homologs to previously reported ESP from other nematodes included a fatty-acid retinoid binding protein (SR02714) (31) and astacin, a metalloproteinase (SR11111), related to the proteases reported for the infective larval stages of related skin-invasive nematodes, such as *S. stercoralis, Ancylostoma caninum,* or *Onchocerca volvulus* (18, 32, 33). The full-length sequences of the *S. ratti* and the *Onchocerca* astacins have first been described by Borchert *et al.* (19). The notion that astacins were secreted was supported by the presence of a canonical signal peptide for secretion sequence. The release of metalloprotease from *S. ratti* iL3 was shown to be completely inhibited by cycloheximide (data not shown), confirming that astacin was indeed actively translated and secreted.

A third example of such ESP homologs was the EST cluster SR00386. BLAST search of this EST cluster identified, as best matching homolog, the third larva (L3)-specific L3NieAg from *S. stercoralis*, which was reported as a highly specific immunodiagnostic antigen of *S. stercoralis* (34) and appears to be weakly related to a group of proteins comprising the secretory vespid venom allergen family. However, the BLAST match was only scored with an E-value of 0.15 indicating either very little homology for this particular protein even between the two related *Strongyloides* species, or that the real ortholog has not yet been sequenced. These facts might indicate that Nie family proteins are possibly genus-specific among the *Strongyloides* spp.

ESP Specific for S. ratti Parasitic Females—In total, 79 proteins were identified solely in the parasitic female ESP. These proteins were assigned to protein digestion and folding ($n = 11$), heat-shock proteins ($n = 3$), carbohydrate metabolism ($n = 4$), nucleic acid metabolism ($n = 17$), structural proteins ($n = 3$), and proteins of other putative functions ($n = 20$). Interestingly, 11 proteins were not assigned to any function or specific protein. Nine of the pF-specific ESPs did not relate to any *S. ratti* or *S. stercoralis* EST clusters, *i.e.* they were not covered by the current *Strongyloides* EST cluster database. Instead, only homologous sequences from other nematodes *e.g. C. elegans, Necator americanus,* and *Heterodera glycines* were identified (see supplemental Table S4).

The 25 highest-scoring pF-specific proteins were listed in Table IIB. One of the most abundant proteins shows homology to a *B. malayi*-derived EF-hand protein family member that had putative calcium-binding activity. Another calcium-binding pF-specific ESP was the secreted protein acidic and rich in cysteine (SPARC), which had been shown to be an extracellular calcium-binding protein (35). The EST cluster corresponding to this SPARC homolog covered the N terminus of the protein and included a predicted a signal peptide for secretion, corroborating the fact that SPARC is *a bone fide* ESP.

Another interesting group of pF-specific proteins were heat shock proteins (HSPs). These included two small HSP proteins (SR00984, SR03349) homologous to proteins from *C. elegans* and the parasitic nematode *T. spiralis*, which was also detected in *Trichinella pseudospiralis*-derived excretome/secretome specimens (36). In addition, a protein with homology to *C. elegans* endoplasmin was identified. The endoplasmins belong to the group of HSPs and were important for the processing and transport of secreted proteins. The human endoplasmin precursor was also termed HSP-90 beta.

One protein function was particularly enriched in the pF-derived E/S proteome compared with the iL3 excretome/secretome, namely protein digestion and folding. The number of proteins assigned to this category increased from 3.6%

TABLE II

A, B, C. The Tables list the 25 highest scoring proteins of E/S products from (A) infective larvae (iL3), (B) parasitic females (pF), and (C) free-living stages (fIS) of S. ratti. The lists include the cluster numbers of S. ratti or S. stercoralis ESTs (Cluster), the highest scoring putative proteins identified in a BLAST search (BLAST alignment), the species in which these proteins occurs (Species), the NCBI protein accession numbers of these proteins (Accession Number, the expectation value (E), the presence of a predicted signal peptide in the proteins (SP), the EST length (EST Lgt.), the percentage coverage (% Cov.), the number of peptides found within the EST cluster sequence (# Pep.) and the unused protein scores (UPS)

Table II A. The 25 highest scoring proteins in the E/S products of S. ratti infective larvae. E, expectation value; SP, signal peptide; Lgt., EST length; % Cov., percentage coverage; # Pep., number of peptides; UPS, unused protein scores

N°.	Cluster	BLAST alignment	Species	Accession number	E	SP	EST Lgt.	% Cov.	# Pep.	UPS
1	SS01511	RAS-related protein RAB-1A	*Brugia malayi*	XP_001901944	$7e^{-104}$	No	205	57.5	8	16.05
2	SR02886	Hypothetical 35.6 kDa protein	*B. malayi*	XP_001899587	$1e^{-71}$	No	180	55.0	7	14.10
3	SR01803	Thiosulfate sulfuryltrans ferase	*B. malayi*	XP_001901653	$1e^{-15}$	No	174	53.4	7	14.03
4	SS00138	Adenylate kinase	*B. malayi*	XP_001894222	$4e^{-62}$	No	149	49.6	6	14.00
5	SR11111	Metalloprotease precursor	*Strongyloides stercoralis*	AAK55800	$2e^{-61}$	Yes	265	43.8	6	13.72
6	SR01001	Myosin-filarial antigen	*B. malayi*	AAB35044	0.0	Truncated	490	41.2	13	13.67
7	SR02558	Lethal family member (let-805)	*Caenorhabditis elegans*	NP_001022641	$1e^{-69}$	Yes	190	37.8	5	13.52
8	SR00386	L3NieAg.01	*S. stercoralis*	AAD46493	0.15	Truncated	112	50.8	5	13.50
9	SR00366	Hypothetical protein DDBD-RAFT_0217849	*Dictyostelium discoi-deum*	XP_642992	$5e^{-08}$	No	190	40.5	6	13.15
10	SR00901	TPR domain containg protein	*B. malayi*	XP_001902724	$5e^{-48}$	No	226	34.9	6	12.73
11	SS02590	Sensory Axon guidance family member	*C. elegans*	NP_001033397	$3e^{-42}$	Yes	169	59.7	6	12.00
12	SR03037	Transthyretin related family member	*C. elegans*	NP_499054	$1e^{-30}$	Yes	147	50.3	5	11.80
13	SR03119	Short chain reductase/ dehydrogenase	*B. malayi*	XP_001900343	$1e^{-46}$	No	179	30.1	5	11.57
14	SS01266	Myosin-4	*C. elegans*	P02566	$3e^{-94}$	No	258	26.0	6	11.45
15	SR00998	Myosin light chain family member	*C. elegans*	NP_510828	$2e^{-73}$	No	170	31.8	4	10.60
16	SR04474	Peptidase family M1 containing protein	*B. malayi*	XP_001897028	$2e^{-64}$	No	196	32.1	4	10.36
17	SR03753	K02D10.1b	*C. elegans*	NP_498936	$5e^{-30}$	No	154	14.3	3	10.05
18	SR02741	Fatty acid retinoid binding protein	*Wuchereria bancrofti*	AAL33794	0.37	No	139	15.8	4	10.02
19	SS01256	Hypothetical protein Bm1_13900	*B. malayi*	XP_001894244	$1e^{-26}$	Yes	228	39.0	5	10.00
20	SR01321	Hypothetical protein Bm1_36850	*B. malayi*	XP_001898817	$1e^{-12}$	No	176	43.2	5	10.00
21	SR00700	Na, K-ATPase alpha subunit	*C. elegans*	AAB02615	$3e^{-101}$	No	233	29.2	4	9.71
22	SR02060	Cell division cycle related family member	*C. elegans*	NP_495705	$3e^{-92}$	No	193	32.6	4	9.50
23	SR03954	CAP protein	*B. malayi*	XP_001891888	$2e^{-53}$	No	242	28.1	4	9.22
24	SS01276	F55F3.3	*C. elegans*	NP_510300	$2e^{-104}$	No	317	12.0	3	9.17
25	SR00383	Propionyl Coenzyme A Carboxylase	*C. elegans*	NP_509293	$2e^{-17}$	No	76	50.0	3	9.10

(7/196) in iL3 to 13.9% (11/79) in pF. Within these 11 proteins, six putative proteases were identified as pF-specific E/S proteins: three metalloproteinases with homologues in *S. stercoralis*, *A. caninum* (37) and *Nasonia vitripennis*, respectively (it should be noted that the metalloproteinases identified as pF-specific differ from the astacin found abundantly in the iL3 E/S proteome fraction (see above)); one aspartyl proteinase-like protein (APR-2); and two EST clusters (SR03191 and SR01641) with pronounced homology to prolyl oligopeptidases (*prolyl serine carboxypeptidase; E.C. 3.4.21.26,* PSC).

ESP Specific for S. ratti Free-living Stages—In the E/S samples derived from the fIS, only 35 stage-specific proteins were identified (supplemental Table S5). Interestingly, two of the 25 highest-scoring ESTs (Table IIC) did not share any significant homology with proteins in the public database ($E < 10^{-5}$). These proteins might not only be stage- but also organism-specific. Another eight proteins showed sequence similarity to hypothetical proteins from *C. elegans*, *C. briggsae,* and/or *B. malayi*, *i.e.* proteins for which not much additional information is available. Taking together the proteins without similarity and the large number of hypothetical proteins highlights the fact that currently, there is very limited knowledge about the functions of the excretome/secretome of free-living stages in *S. ratti*.

Table II B. The highest scoring proteins in the E/S products of S. ratti parasitic females. E, expectation value; SP, signal peptide; Lgt., EST length; % Cov., percentage coverage; # Pep., number of peptides; UPS, unused protein scores

N°.	Cluster	BLAST alignment	Species	Accession number	E	SP	EST Lgt.	% Cov.	# Pep.	UPS
1	SR01608	EF hand family protein	*Brugia malayi*	XP_001901161	$2e^{-37}$	Yes	158	69.0	8	23.28
2	SR03191	Prolyl endopeptidase	*Rattus norvegicus*	EDL99674	$3e^{-19}$	No	189	51.3	6	16.69
3	SR03587	Metalloprotease	*Nasonia vitripennis*	XP_001606489	$9e^{-06}$	Yes	166	42.8	6	14.23
4	SR03901	Aspartyl protease (asp-2)	*C. elegans*	NP_505384	$4e^{-43}$	No	191	56.5	5	13.20
5	SR04847	Acetylcholinesterase 2	*Ditylenchus destructor*	ABQ58116	$1e^{-44}$	No	192	36.5	5	12.4
6	SR03310	mp1	*Onchocerca volvulus*	AAV71152	$2e^{-13}$	Yes	189	39.2	5	11.64
7	SR01641	Prolyl endopeptidase	*Treponema denticola*	NP_971802	$2e^{-12}$	No	126	31.0	4	11.26
8	SR00564	Calumenin	*C. elegans*	NP_001024806	$2e^{-134}$	Yes	286	19.2	4	10.87
9	SR00984	Small heat-shock protein	*Trichinella spiralis*	ABJ55914	$2e^{-21}$	No	160	35.6	4	10.67
10	SR04455	Hypothetical protein CBG05204	*Caenorhabditis briggsae*	XP_001664881	2.0	Yes	88	56.8	5	10.64
11	SR02054	Scavenger receptor cysteine-rich protein	*Culex pipiens quinquefasciatus*	XP_001866937	$3e^{-24}$	Yes	328	14.6	4	10.44
12	SR03349	Heat-shock protein HSP17	*C. elegans*	NP_001023958	$2e^{-20}$	No	157	39.5	5	10.04
13	SR01073	Ribosomal protein (rpl-5)	*C. elegans*	NP_495811	$2e^{-119}$	No	290	19.3	4	9.47
14	SR00396	Endoplasmin precursor	*B. malayi*	XP_001899398	$7e^{-98}$	Yes	231	16.5	3	8.56
15	SR00986	60S ribosomal protein L10	*B. malayi*	XP_001898297	$2e^{-85}$	No	189	17.5	3	8.26
16	SR01297	Immunosuppressive ovarian message protein	*Ascaris suum*	CAK18209	$2e^{-17}$	Yes	324	19.8	4	8.15
17	SR04713	Surface antigen BspA-like	*Trichomonas vaginalis*	XP_001315000	5.3	No	55	89.1	3	7.27
18	SR02663	Metalloprotease precursor	*S. stercoralis*	AAK55800	$6e^{-12}$	Truncated	182	19.2	3	6.91
19	SR01002	Ribosomal protein (rps-18)	*C. elegans*	NP_502794	$5e^{-75}$	No	154	15.6	2	6.64
20	SR00979	Ribosomal protein L9	*Strongyloides papillosus*	ABK55147	$2e^{-73}$	Truncated	166	21.7	2	6.47
21	SR02153	Hypothetical protein CBG20335	*C. briggsae*	CAP37373	$2e^{-34}$	No	178	13.5	2	6.34
22	SR02118	Phosphoribosyl transferase	*B. malayi*	XP_001895434	$2e^{-27}$	No	152	31.6	3	6.24
23	SS03220	Intermediate filament protein (ifa-3)	*C. elegans*	NP_510649	$6e^{-38}$	No	141	24.1	3	6.23
24	SS03344	SPARC precursor	*B. malayi*	XP_001897784	$2e^{-74}$	Yes	175	20.6	3	6.23
25	SR01499	Troponin family protein	*B. malayi*	XP_001898461	$5e^{-50}$	No	257	14.0	3	6.19

The list of flS-specific ESPs featured several hydrolases, including two serine proteases, one aspartic protease, a lysozyme family member and a carbohydrate-hydrolyzing enzyme. One protein (SS00929) showed similarity to a high-mobility group box (HMGB) protein from *C. elegans*. However, it had been shown in *C. elegans* and *B. malayi* that such HMGB proteins were predominantly expressed in developing larvae (38); thus, the identification of this protein might indicate the presence of small amounts of contaminating L1 and L2 larvae in the cultures.

Verification of Stage Relation of S. ratti Proteins by Differential Gene Expression Through qRT-PCR Analysis—Quantitative real-time PCR (qRT-PCR) was used to measure relative transcription levels of 10 selected genes (Table I), whose products, *i.e.* proteins, were found to be of higher abundance in iL3, pF and flSs. These proteins could be analyzed in this experiment. The testing of stage-specific transcripts included (1) *Sr*-astacin (SR11111) and ZK1073.1 (SR02886) for the iL3 stage, (2) *Sr*-PSC-1 (SR01641), *Sr*-calumenin (SR00564), *Sr*-chitin-binding protein (SR04455), *Sr*-trypsin inhibitor-like protein (SR02054), and *Sr*-phosphoribosyl-transferase (SR02118) for the pF stage, and (3) MFP2B (SR00863), *Sr*-CBG22129 or Y51F10 (SR02091), and a *Sr*-lysozyme family protein (SR00671) representing the flS stage. The qRT-PCR results for each transcript were expressed relative to the respective transcript level of the flF stage. As a control, we used proteins that are constantly expressed during the life-cycle: *Sr-gapdh* and actin. The efficiency and linearity of qRT-PCR reactions were examined using 10-fold serial dilutions, indicating efficient amplification. Furthermore, each qRT-PCR reaction was performed on two biological replicates. The qRT-PCR reactions corroborated the findings of the proteomics experiments, *i.e.* increased transcript levels for those proteins that showed exclusive presence in the respective E/S proteome (Fig. 3). One exception was the *Sr*-galectin-2 (*Sr*-GAL-2; SR00627), which was observed in the ESP from all stages, but was found 2.1-fold up-regulated in iL3 whereas another galectin (*Sr*-Gal-1; SS00840) was found up-regulated in flF. In contrast, the phosphoribosyl-transferase (*Sr*-PhRT) was identified as pF-specific. At the transcript level, however, no differential abundance could be measured for *Sr*-PhRT, indicating that the secretion of this protein was post-transcriptionally regulated either at the translational or post-translational level. The transcript levels

Table II C. The highest scoring proteins in the E/S products of S. ratti free-living stages. E, expectation value; SP, signal peptide; Lgt., EST length; % Cov., percentage coverage; # Pep., number of peptides; UPS, unused protein scores

N°.	Cluster	BLAST alignment	Species	Accession number	E	SP	EST Lgt.	% Cov.	# Pep.	UPS
1	SR02994	Hypothetical protein Y49E10.18	*Caenorhabditis elegans*	NP_499623	$2e^{-27}$	Yes	143	51.0	7	19.13
2	SR00863	MFP2b	*Ascaris suum*	AAP94889	$5e^{-71}$	No	173	52.0	7	14.85
3	SR00375	Hypothetical protein CBG05949	*Caenorhabditis briggsae*	XP_001670383	$5e^{-09}$	Yes	148	31.1	5	13.91
4	SR02091	Hypothetical protein CBG22129	*C. briggsae*	XP_001667627	$1e^{-35}$	Yes	174	36.8	6	13.27
5	SR00671	Lysozyme family member (lys-5)	*C. elegans*	NP_502193	$4e^{-37}$	Yes	160	23.1	4	12.70
6	SR02511	Acyl sphingosine amino hydrolase	*C. briggsae*	CAP33700	$2e^{-48}$	Yes	184	27.2	4	8.35
7	SR01169	Aminotransferase	*Clostridium botulinum*	ZP_02614737	0.53	No	176	31.8	4	8.14
8	SR00576	MSP domain protein	*B. malayi*	XP_001899679	$3e^{-32}$	No	97	47.4	4	8.02
9	SR00479	Hexosaminidase B	*Pantroglodytes*	XP_517705	$2e^{-46}$	Yes	167	16.8	2	7.13
10	SR00767	F25A2.1	*C. elegans*	NP_503390	$6e^{-25}$	No	178	17.4	2	6.67
11	SS01173	Enoyl-CoA reductase	*A. suum*	AAC48316	$1e^{-104}$	No	299	10.0	2	6.41
12	SR00821	Saposin-like protein	*C. elegans*	NP_491803	5.4	Yes	86	54.7	3	6.39
13	SR00750	Similar to mannose receptor	*Gallus gallus*	XP_418617	$2e^{-07}$	Yes	174	21.3	3	6.35
14	SR00354	Acid sphingomyelinase	*C. elegans*	NP_001040996	$2e^{-89}$	Yes	269	19.3	3	6.09
15	SR01936	Hypothetical protein CBG21853	*C. briggsae*	XP_001672742	$1e^{-21}$	Yes	190	13.7	2	5.98
16	SR00380	Hypothetical protein EUBVE N 01944	*Eubacterium ventriosum*	ZP_02026680	7.9	Yes	154	14.9	2	5.78
17	SR05257	Putative serine protease F56F10.1	*C. elegans*	P90893	$2e^{-24}$	Yes	185	25.4	2	5.52
18	SR02550	Putative serine protease F56F10.1	*C. elegans*	P90893	$2e^{-35}$	Yes	239	11.7	2	5.22
19	SS01082	Hypothetical 86.9 kDa protein	*B. malayi*	XP_001896095	$5e^{-51}$	No	309	6.8	2	5.22
20	SR02018	Yeast Glc seven-like Phosphatase	*C. elegans*	NP_491237	$2e^{-94}$	No	184	13.0	2	4.74
21	SR00716	F09C8.1	*C. elegans*	NP_510636	$3e^{-45}$	Yes	170	22.4	2	4.66
22	SR01063	Aspartyl protease precursor	*C. briggsae*	CAP30637	$2e^{-98}$	Yes	359	10.9	2	4.49
23	SS00929	High mobility group protein	*C. elegans*	NP_496970	$5e^{-21}$	No	94	20.2	2	4.02
24	SR00223	Hypothetical protein C50B6.7	*C. elegans*	NP_506303	$6e^{-51}$	Yes	192	18.2	2	4.02
25	SR00899	Hypothetical protein CBG09313	*C. briggsae*	XP_001674244	$4e^{-11}$	No	231	13.9	2	4.01

for *Sr*-PhRT—although found as protein only in pF—showed such little variation that it can serve as control.

Immune Recognition of S. ratti Proteins—ELISA was performed to determine if the E/S proteins from iL3, pF and fIS were targets for immune recognition. Sera from 10 rats were taken before and 32 days after subcutaneous infection with 1500 iL3. Furthermore, human sera from two healthy European individuals, *i.e.* from nonendemic area of strongyloidiasis and from ten individuals living in West Africa, *i.e.* an area endemic for the genetically closely related *S. stercoralis* and other intestinal helminths were examined. The ELISA revealed graduated IgG reactivities of sera from both *Strongyloides*-exposed rats and humans, with ESP from pF (high), iL3 (mid), and fIS (low) (Figs. 4*A*, 4*B*; significances varied between $p < 0.05$ and $p < 0.001$).

Identification of Sr-prolyl Serine Carboxypeptidase (PSC-1) Full-Length Gene Sequence—In the pF E/S specimens, we identified several high-scoring pF-specific peptides that were assigned to two ESTs, both showing significant similarity to prolyl oligopeptidase (PSC-1; SR01641 and SR03191; see Table IIB). The *S. ratti* EST database contained a third cluster, SR03122, that had an overlapping N-terminal region with SR03191. Aligning SR01641, SR03191, and SR03122 resulted in a fragment with 454 amino acids (supplemental Fig. S3). The 5′ and 3′ RACE amplification was used to get the full-length *Sr*-PSC-1 cDNA sequence, which was confirmed by cloning and subsequent sequencing. Combining the previously known EST sequences and newly obtained 5′- and 3′ sequences resulted in the first full-length *S. ratti* prolyl oligopeptidase (prolyl serine carboxypeptidase; E.C. 3.4.21.26). The *S. ratti* prolyl oligopeptidase (PSC-1) contains an open reading frame of 2364 nucleotides encoding for a protein of 797 amino acids length and corresponding to a molecular weight of 91 kDa (supplemental Fig. S4; GenBank Accession number FJ011551.1). The protein sequence was added to the search database, and the ProteinPilot searches were repeated. The search identified 25 peptides with a confidence score of 99% and sequence coverage of 32%, resulting in an unused protein score of 65.71. Accordingly, *Sr*-PSC-1 was the highest-scoring pF-specific protein (with the caveat, that PSC-1 was one of the few full-length *S. ratti* proteins in the database used for the protein identification searches). In accordance, *Sr*-PSC-1 was found extremely up-regulated in pF applying the qRT-PCR (Fig. 3).

Sequence Analysis of Sr-PSC-1—Supplemental Fig. S4 shows the full-length nucleotide and amino acid sequence of *Sr*-PSC-1. The yellow nucleotide sequences were the previously unknown residues of *Sr*-PSC-1. Using Prosite, the following features were identified: *Sr*-PSC-1 contained a signal peptide for secretion with the cleavage site between position 22 and 23 (Fig. 5*A*); the main domains of *Sr*-PSC-1 were the Peptidase_S9_N region ranging from amino acid residue 72 to 487 and the serine-active site (SAS) between amino acid

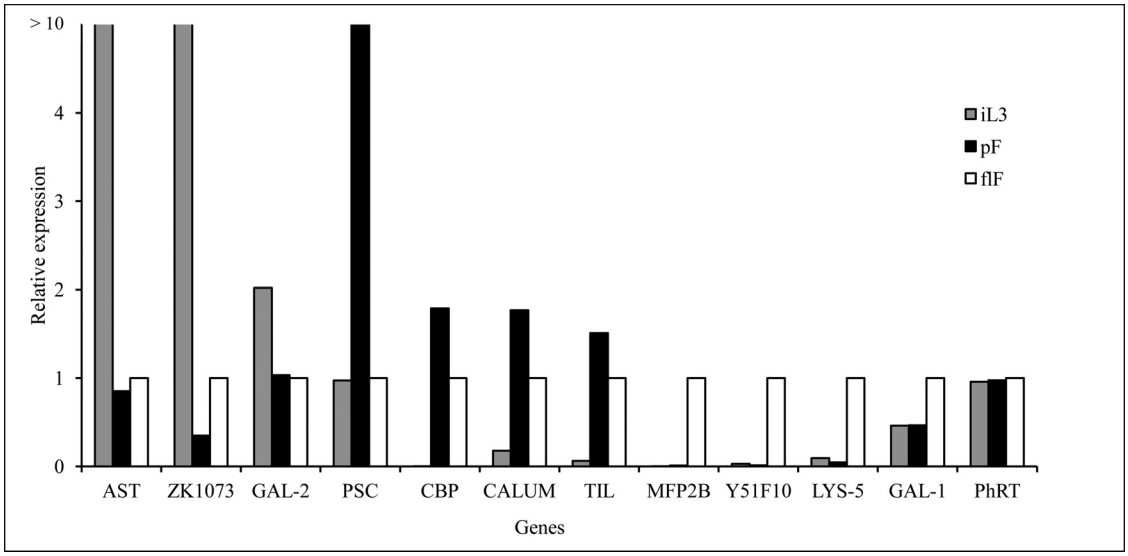

FIG. 3. **Stage-specific gene expression confirming stage-related occurrence of secreted proteins.** The testing of stage-specific transcripts included the genes of *Sr*-astacin (SR11111; AST), ZK1073.1 (SR02886; ZK1073), *Sr*-galectin-2 (SS00627; GAL-2), *Sr*-PSC-1 (SR01641; PSC), *Sr*-chitin-binding protein (SR04455; CBP), *Sr*-calumenin (SR00564; CALUM), *Sr*-trypsin inhibitor-like protein (SR02054; TIL), MFP2B (SR00863), *Sr*-Y51F10.7 or CBG22129 (SR02091; Y51F10), a *Sr*-lysozyme family protein (SR00671; LYS-5), galectin-1 (SS00840; GAL-1), and *Sr*-phosphoribosyl-transferase (SR02118; PhRT). cDNA from infective larvae, parasitic and free-living females were used as a template in real-time quantitative PCR, applying a SYBR Green assay with gene-specific primers. Data were expressed as relative quantity of gene-specific transcription levels of free-living female stage as baseline (value = 1). The results of all samples were normalized to the expression levels of the constitutively expressed gene GAPDH. The experiments were performed twice.

residue 602 and 632 (supplemental Fig. S4, Fig. 5*A*). Aligning and comparing the sequences of 24 different prolyl oligopeptidase up- and downstream of the active-site serine residue identified six conserved amino acid residues (Fig. 5*B*): an aspartic acid residue in the –26 position, an alanine residue in the –21 postion, and glycine residues in the –2, +2, and +3 positions. The corresponding sequence logo can be found in Fig. 5*B*. The active-site serine (Ser627 in *Sr*-PSC-1) is part of the catalytic triad essential for serine proteases, which also includes Asp713 and His753 (39). The residues of this catalytic triad (Ser, Asp, His) are shown in red in supplemental Fig. S4.

Using Swiss Model as protein structure homology-modeling service (template number: 1e5tA) we generated a model for the three-dimensional structure of *Sr*-PSC-1 (Fig. 5*C*) (40). Based on this three-dimensional model, the enzyme is cylindrical and consists of two domains, a peptidase domain and a seven-bladed beta-propeller. The catalytic triad is located in a large cavity at the interface of the two domains. The serine 627 (white) is found at the tip of a sharp turn and directly next to histidine 753 (violet), containing the catalytic imidazole group. The spatially adjacent aspartic acid 713 (yellow) and the histidine 753 are in contact via hydrogen bonds between one of the two oxygen atoms of the carboxylate group and the NH-group of the imidazole ring.

Inhibition of Sr-PSC-1 Enzyme Activity—Based on the finding that *Sr*-PSC-1 is (1) highly expressed (Fig. 3), (2) efficiently secreted, and (3) specific for the parasitic female stage, *Sr*-PSC-1 is potentially very important for drug development as the inhibition of this serine protease might affect relevant proteolytic activities. Prolyl oligopeptidases have recently gained pharma-ceutical interest, because prolyl oligopeptidase inhibitors have been shown to have anti-amnesic properties in rats, increase the brain levels of several neuropeptides (41) and improve cognition (42). We investigated the effect of prolyl oligopeptidase inhibitors on parasitic nematodes, which has never been done before. To this end, we added four different pyrrolidine derivatives (1A, B and 2A, B) (supplemental Fig. S1) (29) to *in vitro* cultures of parasitic females and observed their motility as proxy for their health status. All treated worms showed a dose-dependent decrease in motility when compared with the nontreated control group within 30 to 60 min of adding the prolyl oligopeptidase inhibitors (Fig. 6). The inhibitor compounds 2A and 2B were much more effective than the compounds 1A and 1B (29). The prolyl oligopeptidase inhibitor-induced change in motility was not reversible as replacing the culture medium with fresh medium without the inhibitors 18 h after the treatment did not result in recurrence of the motility confirming that motility is a good proxy for mortality.

DISCUSSION

E/S products (ESPs) secreted by cells and organisms play pivotal biological roles across a wide range of parasitic organisms. Representing the primary interface between the parasite and the host, the E/S components include proteins involved in biological processes like cell migration, cell adhesion, cell-cell communication, proliferation, differentiation, morphogenesis,

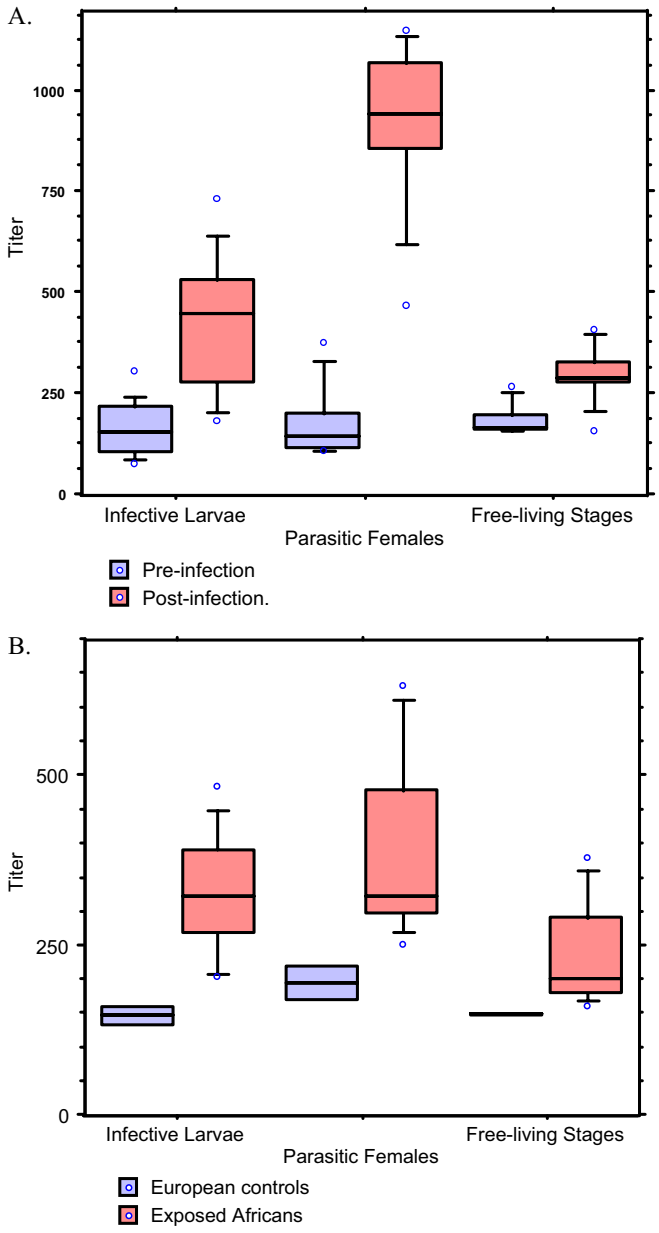

FIG. 4. **Demonstration of IgG antibody reactivity with proteins in E/S products from iL3, pF and fIS using sera from rats (*A*) and humans (*B*).** ELISA titers—shown as box plots and quartiles—obtained (*A*) for 10 sera before (pre) and 32 days after (post) infection with *S. ratti* and (*B*) for two nonexposed Europeans not exposed to *S. stercoralis* and 10 Africans exposed to or infected with *S. stercoralis*. The antibody titers differed significantly (Mann-Whitney *U* test: $p < 0.05$ - $p < 0.001$) within the two respective groups of rat sera (for iL3: $p < 0.001$, pF: $p < 0.001$ and for fls: $p < 0.05$) and human sera for E/S products from iL3 and pF and fIS ($p < 0.05$ for all).

and the regulation of immune responses (43). We have undertaken the proteomic study of *S. ratti* as model organism to investigate the parasite-host interactions in parasitic nematode infections. Accordingly, we aimed to provide insights into the E/S proteome of *S. ratti* and the interplay of the excretome/secretome with the development of *S. ratti* which has a complex life cycle with free-living stages, each having unique roles in host-pathogen interactions. In fact, for the entire genus *Strongyloides*, only a single proteomic study has been published (44). To this end, we isolated E/S specimens from three distinct developmental stages: iL3, pF, and fIS.

Prior to starting this endeavor we showed that the proteins present in the culture supernatant are indeed caused by secretion and not because of leakage of dead or damaged cells. Interestingly, the pattern of protein bands differed strongly between ESPs and somatic crude extracts of the stages (supplemental Fig. S2). Furthermore, a rank-order correlation of the identified ESP and extract proteins indicated little to no rank-order correlation, thus providing further evidence in support of secretion and against worm lysis. We applied cycloheximide, a potent inhibitor of protein translation, in the iL3 cultures. In addition, we used azide treatment and exposure to unphysiological conditions at 4 °C and 70 °C. The almost complete reduction of proteins in the supernatant and also the disappearance of the astacin metalloproteinase, which was the most prominent proteolytic component in the gelatin gels, confirmed *bona fide* excretion/secretion and excluded leakage and/or random lysis as reason for observing the identified proteins. This validation experiment was important, as our analysis identified numerous proteins normally considered as cytosolic or nuclear. However, recent studies have shown that many proteins, including peroxidoxin, galectins, heat shock proteins, and high-mobility group box 1, were indeed excreted and secreted proteins (45–47).

Once we confirmed that excretion and secretion was the cause for observing the proteins in the supernatant, we used SDS-PAGE in combination with LC/MS (GeLC/MS) for a comprehensive analysis of the different excretomes/secretomes during *S. ratti* development. In total 586 ESPs were identified. Our study is the first proteomic study of *S. ratti*-derived specimens and furthermore is the largest proteomic study in the genus *Strongyloides* by far. Previously, only a single proteomic study of *Strongyloides*-derived samples been published and this study identified merely 26 proteins (44).

Any proteomic study in *Strongyloides* (or many other parasitic nematodes) is hampered by the limited availability of protein sequence information. However, the use of available protein and EST sequences from *S. ratti* and *S. stercoralis* (combined with other nematodes) and new technologies can partially overcome the problems associated with lack of organism-specific sequence information. For instance, new search engines, such as ProteinPilot, allow for database-wide substitutions during the protein identification search. Thus, despite this lack of sequence information we did generate the second largest nematode E/S proteome map to date. The only larger nematode E/S study was recently published by Bennuru *et al.* (13) who studied the *B. malayi* E/S proteome and profited from the availability of the complete genome sequence (48).

Proteins from a wide range of biological processes and functions were identified in our study including cell migration,

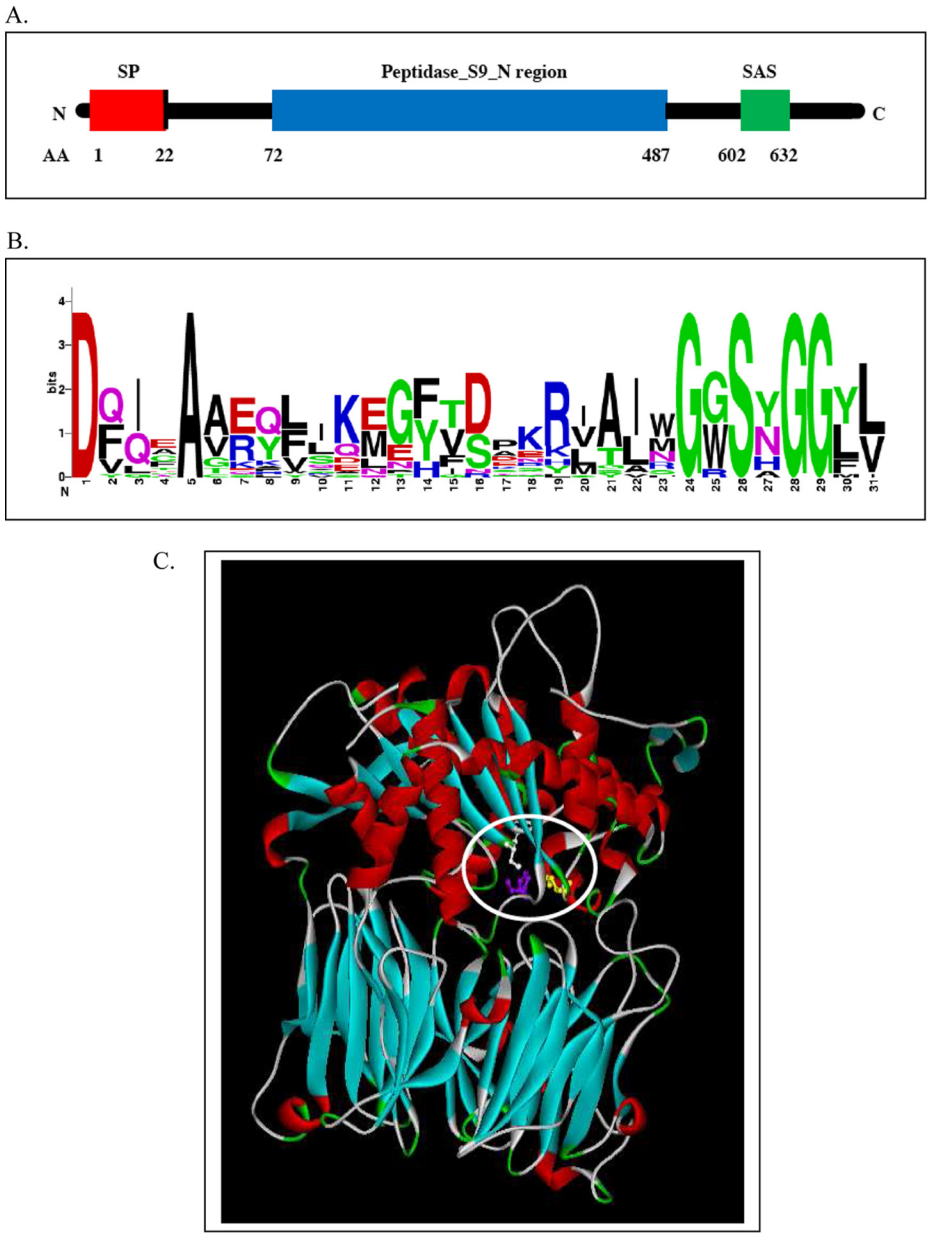

FIG. 5. ***A*, Domain structure of the *Sr*-PSC-1. AA, amino acid; SP, signal peptide; SAS, serine active site.** *B*, Sequence logo of the serine active site generated from multiple sequence alignments of 24 different prolyl oligopeptidase active sites. The total height of a logo position depends on the degree of conservation in the corresponding multiple sequence alignment column. Highly conserved alignment columns produce high logo positions. The tallest letters of six amino acids (D, A, G, S, G, G) correspond to the most conserved amino acids which are underlined in the sequence shown in the supplemental Fig. S4 (source http://us.expasy.org/cgi-bin/prosite). *C*, Ribbon diagram of *Sr*-PSC-1. The peptidase domain is located in the upper region, the β-propeller domain in the lower region. a) light blue - β-propeller structures, b) red - helical structures, c) white - Ser627, d) violet - His753, e) yellow - Asp713.

cell adhesion, cell-cell communication, proliferation, differentiation, morphogenesis, and the regulation of immune responses. In addition, numerous proteins of unknown function and hypothetical proteins were found. For the subsequent analysis of stage-specific E/S proteins, we did not attempt any detailed quantitative analysis of the identified proteins. Instead, we followed a stringent binary observed/not observed approach.

Recently, a microarray with 2,227 putative genes was used to identify genes likely to play a key role in the parasitic life of *S. ratti* (49). In this report, the microarray was probed with cDNA prepared from parasites subjected to low or high immune pressures, *i.e.* harvested 6 and 15 days postinfection, respectively. Comparison of these transcript expression data with our proteomic data identified several proteins which were specific for a particular stage or were expressed in two or three studied stages. For example, the cluster SR00984, which relates to a small heat-shock protein (HSP), is only observed as an ESP in pF-derived specimens and as an actively transcribed gene. Of note, the only stage-specific excreted and secreted heat shock proteins were found in the pF-derived specimens (50). In addition, numerous other non-stage specific HSPs were identified, including the abundant *Sr*-HSP-10 and *Sr*-HSP-60 proteins, which were recently partially characterized (17).

The stage-specific transcripts from the free-living and parasitic stages, which were also observed in the qRT-PCR of selected *S. ratti* genes, confirmed the stage-specific expres-

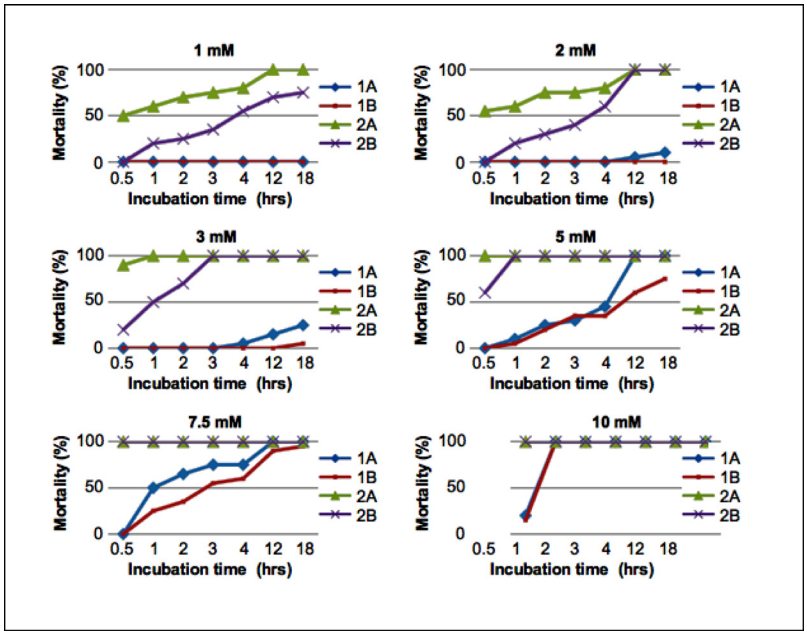

FIG. 6. **Effect of different prolyl oligopeptidase inhibitors during *in vitro* culture of *S. ratti* parasitic female worms.** Single graphs show different concentrations of compounds 1 (blue line, diamonds), 2 (red line, circles), 3 (green line, triangles), and 4 (purple line, x's). The mortality represents the percentage of worms that do not show any movements at a certain time point. The inhibitors included are: (1A) isophthalic acid 2(S)-(cyclopentanecarbonyl)-pyrrolidine-L-prolyl-2(S)-cyanopyrrolidine amide; (1B) iso-phthalic acid 2(S)-(cyclopentanecarbonyl) pyrrolidine-L-prolyl-2(S)-(hydroxy-acetyl)-pyrrolidine amide; (2A) 4-phenylbutanoyl-L-prolyl-pyrrolidine; (2B) 4-phenyl-butanoyl-L-prolyl-2(S)-cyanopyrrolidine (56).

sion found in the proteomic data. One notable exception was PhRT, which was identified only in the pF sample using proteomics, but showed equal transcript levels throughout *S. ratti* developmental stages. A possible explanation for this observation is that although the majority of the stage-specific ESPs are controlled at the transcriptional level, the excretion and secretion of PhRT is controlled post-transcriptionally, *i.e.* by timed translation or by post-translational events, such as stage-specific post-translational modifications. The remarkable diversity of the expression levels of the various genes in the iL3, pF, and flF, as determined in our study, reflects changes associated with the transition to parasitic lifestyle and the adaptation to the host. These include the iL3-specific *Sr* astacin (*Sr*-AST), which is homologous to a promising vaccine candidate against the hookworm infections (51). The astacin-like metalloprotease *Ac*-MTP-1 (32) is specifically secreted by the iL3 of the hookworm, showing the same stage specificity as *Sr*-AST (SR11111) in our study. Work from our laboratory had characterized a homologous astacin in the filaria *O. volvulus* (19). The *Sr*-AST identified in the iL3 specimens corresponded to a full-length astacin metalloproteinase sequence that was identified in our laboratory based on a homologous *S. stercoralis* sequence (19). It was interesting to note that this metalloprotease showed elevated expression in iL3 stages of both *S. ratti* and *S. stercoralis* (32), thus underlining its putative role to facilitate skin penetration at the initiation of infection. Besides the iL3-specific astacin, two other EST clusters (SR03587 and SR02663) were identified that showed similarities to astacins. However, these two astacins were pF-specific, thus indicating that different astacins were expressed during different developmental stages. These results show protease activities tailored to the needs of each life cycle stage.

S. ratti prolyl oligopeptidase Sr-PSC-1 is another example of a stage-specific protease that has been exclusively identified in parasitic females. This protein was only partially covered by the EST clusters used for the protein identification. For further characterization of this protein, we cloned the full-length gene; its characteristics are shown in supplemental Fig. S4 and in Fig. 5. *Sr*-PSC-1 represents a typical serine protease characterized by the conserved catalytic triad (aaSer, aaAsp and aaHis). A homolog of *Sr*-PSC-1 with 37% identity with the whole protein was found in *B. malayi*, but shared only 52% identity with the C-terminal region that contained the catalytic domain (www.nematodes-.org/downloads/databases/). In contrast, no significant similarity on a primary sequence level was found with the nonparasitic nematode *C. elegans,* which was unusual because a majority of proteins were commonly shared between *C. elegans* and other nematode species. This may suggest that this protease played a role in parasite establishment within the host, a notion that was supported by the observation that a similar stage-specific gene expression for PSC-1 had been reported before in *Teladorsagia circumcincta* (52). The stage-specificity of PSC-1 in *S. ratti* was supported by the fact that the ESTs encoding PSC-1 originated only from the EST libraries generated from pF. In addition, the comparative PCR analysis (Fig. 3) only showed a positive result for parasitic female cDNA. Interestingly, the EST cluster SR04440, which in the present study occurred in the extracts of pF (data not shown), was also found in a microarray analysis in samples from pF under high-immune pressure (49). The *Strongyloides* PSC-1 represents a novel abundant stage-specific protein that might have relevance for the containment of parasitism.

The serine proteases of the prolyl oligopeptidase family were previously reported in the protozoan parasites *Trypano-*

soma brucei and *Leishmania major* (29). In these parasites, the prolyl oligopeptidase was likely to be involved in host cell invasion and hydrolysis of host proteins (53, 54). Prolyl oligopeptidase had also been studied as a potential therapeutic agent for the treatment of celiac sprue, an inflammatory disease of the small intestine (55). In vertebrates, prolyl oligopeptidase activity had been found throughout the body, with a highest concentration within the brain (56). The prolyl oligopeptidase family S9 was comprised of beta-hydrolase enzymes also sharing the classical catalytic triad. The 80-kDa prolyl oligopeptidase were able to hydrolyze the peptide bond on the carboxyl side of internal proline residues. Evaluation of the sequence data from parasitic *S. ratti* females revealed that the culture supernatants contained sequences matching EST clusters SR01641 and SR03191 that showed homology to prolyl oligopeptidase (22).

Prolyl oligopeptidase had been studied in human and mouse in the context of their neurological roles. The high occurrence of prolyl oligopeptidase in the brain suggested that it was involved in the maturation and degradation of peptide hormones and neuropeptides, such as substance P, oxytocin, and angiotensin. Published data describe different prolyl oligopeptidase inhibitors, that are active *in vitro* and *in vivo* in humans and rodents and increase levels of several neuropeptides in the brain (57). When testing for the effects of several pyrrolidine-derived prolyl oligopeptidase inhibitors on *S. ratti* parasitic females, we observed a clear concentration- and time-dependent reduction in motility (Fig. 6), which was used in the present study as proxy for vitality status of *S. ratti*. This observation might lead to novel treatment options for strongyloidasis.

A variety of proteins that we have identified in the *S. ratti* ESP are homologous to proteins from other nematode species that may have been involved in either the containment of parasitism or the suppression or induction of host-immune responses. These included anti-oxidative proteins (thioredoxin peroxidase, glutathione peroxidase, superoxide dismutase), various proteinases, serpin, galectins, small HSPs, and macrophage migration inhibitory factor (50,58). Rats infected by *S. ratti* form a marked immunity against a challenge infection when immunized with ESP fraction from adult worms (59). Thus, ESP from pF can influence the host defense system. *S. ratti* infection was shown to induce transient nematode-specific Th2 response characterized by the generation of interleukin-4, -5, and -13 that foster eosinophilic granulocytes and mast cells and induce IgG4 and IgE antibody isotype production, which were involved in effector responses (60). Interestingly, ESP from pF were found to be strongly recognized by IgG in sera from *S. ratti*-infected rats and *Strongyloides*-exposed persons living in Africa, whereas ESP from iL3 showed a lower reactivity and ESP from fIS were hardly recognized (Fig. 4).

Although the main focus of our study was the identification of stage-specific ESPs, analyzing the list of commonly found ESPs was also very revealing. Proteins abundantly observed in all three investigated developmental stages were—among others—HSPs, galectins, and proteins involved in oxidative phosphorylation, carbohydrate synthesis and metabolism, biosynthesis, developmental processes, sugar- and fatty acid-binding (supplemental Table S2). In addition, similar to the findings in previous studies of the excretomes/secretomes of parasitic nematodes, we identified several homologous structural proteins such as actin, profiling, or myosin (1, 13, 43, 61–63). Furthermore, we identified tropomyosin, a fibrillar protein involved in the contraction of muscle cells, in the stage independent E/S product. The identification of tropomyosin as an E/S product was not unprecedented, as proteins from the tropomyosin family were also detected in the secretions of adult *B. malayi* stages (61) and *S. mansoni* cercariae (64). Similarly, Hartmann *et al.* (65) showed that birds are partially protected after infection with *A. viteae* infective larvae (iL3) infection when immunized with recombinant tropomyosin. Thus, it can be concluded that the tropomyosin is a widely occurring allergen excreted/secreted by numerous tissue- and intestine-dwelling nematodes (66).

In the present study, almost 600 proteins were identified in the E/S products derived from different developmental stages of *S. ratti*. Half of the E/S products were found in two stages, the largest number (>33%) in iL3 and 13% in pF. Individual parasitic stage-specific proteins were expected to exhibit important biological functions in the general, as well as stage-specific parasite-host-interaction and may reveal immunomodulatory activities, which are of relevance for both the parasite in its mucosal habitat and for the infested host (67). A biological role for the iL3-secreted astacin, the Nie antigen and a fatty acid retinoid binding protein, parasitic female-released prolyl oligopeptidase, small heat shock proteins, and a secreted acidic and rich in cysteine-related protein may be anticipated. These identified proteins include putative immunemodulators that will strengthen research aimed to develop novel intervention tools to control the parasite and prevent the diseases.

Acknowledgments—We thank Dr. G. Pluschke (Department Medical Parasitology and Infection Biology, Swiss Tropical and Public Health Institute, Basel, Switzerland) for providing the *S. ratti* cycle. We thank Dr. Elina M. Jarho (Department of Pharmaceutical Chemistry, University of Kuopio, Finland) for providing the prolyl oligopeptidase inhibitors. The expert assistance of Mrs. K. Krausz and M. Lintzel (Bernhard Nocht Institute), Dr. Christina M. Taylor (The Genome Institute, Washington University School of Medicine, St. Louis), and Zachary Waldon, Peter Warren and Yin Yin Lin (The Proteomics Center at Children's Hospital Boston) is appreciated. We acknowledge the support of Dr. Peter U. Fischer (Department of Internal Medicine, Infectious Diseases Division, Washington University School of Medicine, St. Louis, USA) in the data analysis and helpful discussion. We thank Dr. J. Paulo (The Proteomics Center at Children's Hospital Boston) for critical reading the manuscript. Data of this work form major parts of the doctoral theses by Soblik H and Younis, A. E. in the Faculty of Natural Sciences of the University of Hamburg, Germany.

* This work was supported by the Leibniz Association and the Vereinigung der Freunde des Tropeninstituts Hamburg, the Boehringer Ingelheim Fonds (H. S.), the Egyptian Ministry of Higher Education (A. E. Y.) and the NIH-NIAID support (M. M.).

[S] This article contains supplemental Figs. S1 to S4 and Tables S1 to S5.

¶¶ To whom correspondence should be addressed: NB: Department of Molecular Medicine, Bernhard Nocht Institute for Tropical Medicine, Bernhard-Nocht Strasse 74, 20359 Hamburg, Germany. Tel.: +49-040-42818530; Fax: +49-040-42818400; E-mail: nbrattig@bni-hamburg.de. HS: Proteomics Center at Children's Hospital Boston, Dept. of Pathology, 320 Longwood Ave, Boston, MA 02115, USA. Tel.: +1-617-919-2629; Fax: +1-617-730-0168; E-mail: hanno.steen@childrens.harvard.edu.

|||| These authors contributed equally to the work.

REFERENCES

1. Nagaraj, S. H., Gasser, R. B., and Ranganathan, S. (2008) Needles in the EST haystack: large-scale identification and analysis of excretory-secretory (ES) proteins in parasitic nematodes using expressed sequence tags (ESTs). *PLoS Negl. Trop. Dis.* **2,** e301
2. Hewitson, J. P., Grainger, J. R., and Maizels, R. M. (2009) Helminth immuno regulation: the role of parasite secreted proteins in modulating host immunity. *Mol. Biochem. Parasitol.* **167,** 1–11
3. Woolhouse, M. E., Webster, J. P., Domingo, E., Charlesworth, B., and Levin, B. R. (2002) Biological and biomedical implications of the co-evolution of pathogens and their hosts. *Nat. Genet.* **32,** 569–577
4. Rook, G. A. (2007) The hygiene hypothesis and the increasing prevalence of chronic inflammatory disorders. *Trans. R. Soc. Trop. Med. Hyg.* **101,** 1072–1074
5. Viney, M. E. (2006) The biology and genomics of *Strongyloides*. *Med. Microbiol. Immunol.* **195,** 1–6
6. Grove, D. I. (1996) Human strongyloidiasis. *Adv. Parasitol.* **38,** 251–309
7. Keiser, P. B., and Nutman, T. B. (2004) *Strongyloides stercoralis* in the immuno compromised population. *Clin. Microbiol. Rev.* **17,** 208–217
8. Olsen, A., van Lieshout, L., Marti, H., Polderman, T., Polman, K., Steinmann, P., Stothard, R., Thybo, S., Verweij, J. J., and Magnussen, P. (2009) Strongyloidiasis – the most neglected of the neglected tropical diseases? *Trans. R. Soc. Trop. Med. Hyg.* **103,** 967–972
9. Marcos, L. A., Terashima, A., Dupont, H. L., and Gotuzzo, E. (2008) *Strongyloides* hyperinfection syndrome: an emerging global infectious disease. *Trans. R. Soc. Trop. Med. Hyg.* **102,** 314–318
10. Montes, M., Sawhney, C., and Barros, N. (2010) *Strongyloides stercoralis*: there but not seen. *Curr. Opin. Infect. Dis.* **23,** 500–504
11. Kramme, S., Nissen, N., Soblik, H., Erttmann, K., Tannich, E., Fleischer, B., Panning, M., and Brattig, N. W. (2010) Novel real-time PCR for the universal detection of *Strongyloides* spp. *J. Med. Microbiol*. **60**, 454–458
12. Lok, J. B. (2007) *Strongyloides stercoralis:* a model for translational research on parasitic nematode biology. *WormBook.* **17,** 1–18
13. Bennuru, S., Semnani, R., Meng, Z., Ribeiro, J. M., Veenstra, T. D., and Nutman, T. B. (2009) *Brugia malayi* excreted/secreted proteins at the host/parasite interface: stage- and gender-specific proteomic profiling. *PLoS Negl. Trop. Dis.* **3,** e410
14. Keiser, J., Thiemann, K., Endriss, Y., and Utzinger, J. (2008) *Strongyloides ratti:* in vitro and *in vivo* activity of tribendimidine. *PLoS Negl. Trop. Dis.* **2,** e136
15. Viney, M. E., and Lok, J. B. (2007) *Strongyloides* spp. *WormBook.* **23,** 1–15
16. Whitehead, A. G., and Hemming, J. R. (1965) A comparison of some quantitative methods of extracting small vermiform nematodes from soil. *Ann. Appl. Biol.* **55,** 25–38
17. Tazir, Y., Steisslinger, V., Soblik, H., Younis, A. E., Beckmann, S., Grevelding, C. G., Steen, H., Brattig, N. W., and Erttmann, K. D. (2009) Molecular and functional characterisation of the heat shock protein 10 of *Strongyloides ratti. Mol. Biochem. Parasitol.* **168,** 149–157
18. McKerrow, J. H., Pino-Heiss, S., Lindquist, R., and Werb, Z. (1985) Purification and characterization of an elastinolytic proteinase seceted by cercariae of *Schistosoma mansoni. J. Biol. Chem.* **260,** 3703–3707
19. Borchert, N., Becker-Pauly, C., Wagner, A., Fischer, P., Stöcker, W., and Brattig, N. W. (2007) Identification and characterization of onchoastacin, an astacin-like metalloproteinase from the filaria *Onchocerca volvulus. Microbes Infect.* **9,** 498–506
20. Renard, B. Y., Kirchner, M., Monigatti, F., Ivanov, A. R., Rappsilber, J., Winter, D., Steen, J. A., Hamprecht, F. A., and Steen, H. (2009) When less can yield more - Computational preprocessing of MS/MS spectra for peptide identification. *Proteomics* **9,** 4978–4984
21. Renard, B. Y., Timm, W., Kirchner, M., Steen, J. A., Hamprecht, F. A., and Steen, H. (2010) Estimating the confidence of peptide identifications without decoy databases. *Anal Chem.* **82,** 4314–4318
22. Mitreva, M., McCarter, J. P., Martin, J., Dante, M., Wylie, T., Chiapelli, B., Pape, D., Clifton, S. W., Nutman, T. B., and Waterston, R. H. (2004) Comparative genomics of gene expression in the parasitic and free-living nematodes *Strongyloides stercoralis* and *Caenorhabditis elegans. Genome Res.* **14,** 209–220
23. Martin, J., Abubucker, S., Wylie, T., Yin, Y., Wang, Z., and Mitreva, M. (2009) Nematode.net update 2008: improvements enabling more efficient data mining and comparative nematode genomics. *Nucleic Acids Res.* **37,** D571–578
24. Bendtsen, J. D., Nielsen, H., von Heijne, G., and Brunak, S. (2004) Improved prediction of signal peptides: SignalP 3.0. *J. Mol. Biol.* **340,** 783–795
25. Pfaffl, M. W. (2001) A new mathematical model for relative quantification in real-time RT-PCR. *Nucleic Acids Res.* **29,** e45
26. Livak, K. J., and Schmittgen, T. D. (2001) Analysis of relative gene expression data using realtime quantitative PCR and the 2(-Delta Delta C(T)) method. *Methods* **25,** 402–408
27. Mpagi, J. L., Büttner, D. W., Tischendorf, F. W., Erttmann, K. D., and Brattig, N. W. (2000) Humoral responses to a secretory *Onchocerca volvulus* protein: differences in the pattern of antibody isotypes to recombinant Ov20/OvS1 in generalized and hyperreactive onchocerciasis. *Parasite Immunol.* **22,** 455–460
28. Tischendorf, F. W., Brattig, N. W., Büttner, D. W., Pieper, A., and Lintzel, M. (1996) Serum levels of eosinophil cationic protein, eosinophil-derived neurotoxin and myeloperoxidase in infections with filariae and schistosomes. *Acta Trop.* **62**, 171–182
29. Venäläinen, J. I., Juvonen, R. O., and Männistö, P. T. (2004) Evolutionary relationships of the prolyl oligopeptidase family enzymes. *Eur. J. Biochem.* **271,** 2705–2715
30. Jacob, J., Vanholme, B., Haegeman, A., and Gheysen, G. (2007) Four transthyretin-like genes of the migratory plant-parasitic nematode *Radopholus similis*: members of an extensive nematode-specific family. *Gene* **402,** 9–19
31. Mpagi, J. L., Erttmann, K. D., and Brattig, N. W. (2000) The secretory *Onchocerca volvulus* protein OvS1/Ov20 exhibits the capacity to compete with serum albumin for the host's long-chain fatty acids. *Mol. Biochem. Parasitol.* **105,** 273–279
32. Gomez Gallego, S., Loukas, A., Slade, R. W., Neva, F. A., Varatharajalu, R., Nutman, T. B., and Brindley, P. J. (2005) Identification of an astacin-like metalloproteinase transcript from the iL3 of *Strongyloides stercoralis. Parasitol. Int.* **54,** 123–133
33. Williamson, A. L., Lustigman, S., Oksov, Y., Deumic, V., Plieskatt, J., Mendez, S., Zhan, B., Bottazzi, M. E., Hotez, P. J., and Loukas, A. (2006) *Ancylostoma caninum* MTP-1, an astacin-like metalloprotease secreted by infective hookworm larvae is involved in tissue migration. *Infect. Immun. 7* **4,** 961–967
34. Ravi, V., Ramachandran, S., Thompson, R. W., Andersen, J. F., and Neva, F. A. (2002) Characterization of a recombinant immunodiagnostic antigen (NIE) from *Strongyloides stercoralis* L3-stage larvae. *Mol. Biochem. Parasitol.* **125,** 73–81
35. Schwarzbauer, J. E., Musset-Bilal, F., and Ryan, C. S. (1994) Extracellular calcium-binding protein SPARC/osteonectin in *Caenorhabditis elegans. Methods Enzymol.* **245,** 257–270
36. Ko, R. C., and Fan, L. (1996) Heat shock response of *Trichinella spiralis* and *T. pseudospiralis. Parasitology* **112**, 89–95
37. Feng, J., Zhan, B., Liu, Y., Liu, S., Williamson, A., Goud, G., Loukas, A., and Hotez, P. (2007) Molecular cloning and characterization of Ac-MTP-2, an astacin-like metalloprotease released by adult *Ancylostoma caninum. Mol. Biochem. Parasitol.* **152,** 132–138
38. Jiang, L. I., and Sternberg, P. W. (1999) An HMG1-like protein facilitates Wnt signaling in *Caenorhabditis elegans. Genes Dev.* **13,** 877–889
39. Szeltner, Z., and Polgár, L. (2008) Structure, function and biological relevance of prolyl oligopeptidase. *Curr. Protein. Pept. Sci.* **9,** 96–107

40. Arnold, K., Bordoli, L., Kopp, J., and Schwede, T. (2006) The SWISS-MODEL Workspace: A web-based environment for protein structure homology modelling. *Bioinformatics* **22,** 195–201
41. Atack, J. R., Suman-Chauhan, N., Dawson, G., and Kulagowski, J. J. (1991) *In vitro* and *in vivo inhibition of prolyl endopeptidase. Eur. J. Pharmacol.* **205**, 157–163
42. Schneider, J. S., Giardiniere, M., and Morain, P. (2002) Effects of the prolyl endopeptidase inhibitor S 17092 on cognitive deficits in chronic low dose MPTP-treated monkeys. *Neuropsychopharmacol* **26,** 176–182
43. Maizels, R. M., and Yazdanbakhsh, M. (2003) Immune regulation by helminth parasites: cellular and molecular mechanisms. *Nat. Rev. Immunol.* **3,** 733–744
44. Marcilla, A., Sotillo, J., Pérez-Garcia, A., Igual-Adell, R., Valero, M. L., Sánchez-Pino, M. M., Bernal, D., Muñoz-Antolí, C., Trelis, M., Toledo, R., and Esteban, J. G. (2010) Proteomic analysis of *Strongyloides stercoralis* L3 larvae. *Parasitology* **137,** 1577–1583
45. Rubartelli, A., and Lotze, M. T. (2007) Inside, outside, upside down: damage-associated molecular-pattern molecules (DAMPs) and redox. *Trends Immunol.* **28,** 429–436
46. Robinson, M. W., Hutchinson, A. T., Donnelly, S., and Dalton, J. P. (2010) Worm secretory molecules are causing alarm. *Trends Parasitol.* **26,** 371–372
47. Robinson, M. W., Hutchinson, A. T., Dalton, J. P., and Donnelly, S. (2010) Peroxiredoxin: a central player in immune modulation. *Parasite Immunol.* **32,** 305–313
48. Ghedin, E., Wang, S., Spiro, D., Caler, E., Zhao, Q., Crabtree, J., Allen, J. E., Delcher, A. L., Guiliano, D. B., Miranda-Saavedra, D., Angiuoli, S. V., Creasy, T., Amedeo, P., Haas, B., El-Sayed, N. M., Wortman, J. R., Feldblyum, T., Tallon, L., Schatz, M., Shumway, M., Koo, H., Salzberg, S. L., Schobel, S., Pertea, M., Pop, M., White, O., Barton, G. J., Carlow, C. K., Crawford, M. J., Daub, J., Dimmic, M. W., Estes, C. F., Foster, J. M., Ganatra, M., Gregory, W. F., Johnson, N. M., Jin, J., Komuniecki, R., Korf, I., Kumar, S., Laney, S., Li, B. W., Li, W., Lindblom, T. H., Lustigman, S., Ma, D., Maina, C. V., Martin, D. M., McCarter, J. P., McReynolds, L., Mitreva, M., Nutman, T. B., Parkinson, J., Peregrin-Alvarez, J. M., Poole, C., Ren, Q., Saunders, L., Sluder, A. E., Smith, K., Stanke, M., Unnasch, T. R., Ware, J., Wei, A. D., Weil, G., Williams, D. J., Zhang, Y., Williams, S. A., Fraser-Liggett, C., Slatko, B., Blaxter, M. L., and Scott, A. L. (2007) Draft genome of the filarial nematode parasite *Brugia malayi. Science* **317,** 1756–1760
49. Thompson, F. J., Barker, G. L., Hughes, L., and Viney, M. E. (2008) Genes important in the parasitic life of the nematode *Strongyloides ratti. Mol. Biochem. Parasitol.* **158,** 112–119
50. Younis, A. E., Geisinger, F., Ajonina-Ekoti, I., Soblik, H., Steen, H., Mitreva, M., Erttmann, K. D., Perbandt, M., Liebau, E., and Brattig, N. W. (2011) Stage-specific excretory-secretory small heat shock proteins from the parasitic nematode *Strongyloides ratti* – putative links to host's intestinal mucosal defense system. *FEBS J.* **278,** 3319–3336
51. Hotez, P. J., Ashcom, J., Zhan, B., Bethony, J., Loukas, A., Hawdon, J., Wang, Y., Jin, Q., Jones, K. C., Dobardzic, A., Dobardzic, R., Bolden, J., Essiet, I., Brandt, W., Russell, P. K., Zook, B. C., Howard, B., and Chacon, M. (2003) Effect of vaccination with a recombinant fusion protein encoding an astacinlike metalloprotease (MTP-1) secreted by host-stimulated *Ancylostoma caninum* third-stage iL3. *J. Parasitol.* **89,** 853–855
52. Nisbet, A. J., Redmond, D. L., Matthews, J. B., Watkins, C., Yaga, R., Jones, J. T., Nath, M., and Knox, D. P. (2008) Stage-specific gene expression in *Teladorsagia circumcincta* (Nematoda: Strongylida) iL3 and early parasitic stages. *Int.* J. Parasitol. **38,** 829–838
53. Grellier, P., Vendeville, S., Joyeau, R., Bastos, I. M., Drobecq, H., Frappier, F., Teixeira, A. R., Schrével, J., Davioud-Charvet, E., Sergheraert, C., and Santana, J. M. (2001) *Trypanosoma cruzi* prolyl oligopeptidase Tc80 is involved in nonphagocytic mamalian cell invasion by trypomastigotes. *J. Biol. Chem.* **276,** 47078–47086
54. Bastos, I. M., Motta, F. N., Charneau, S., Santana, J. M., Dubost, L., Augustyns, K., and Grellier, P. (2010) Prolyl oligopeptidase of *Trypanosoma brucei* hydrolyzes native collagen, peptide hormones and is active in the plasma of infected mice. *Microbes Infect.* **12,** 457–466
55. Ehren, J., Govindarajan, S., Morón, B., Minshull, J., and Khosla, C. (2008) Protein engineering of improved prolyl endopeptidases for celiac sprue therapy. *Protein Eng. Des. Sel.* **21,** 699–707
56. Irazusta, J., Larrinaga, G., Gonzáles-Maesto, J., Gil, J., Meana, J. J., and Casis, L. (2002) Distribution of prolyl endopeptidase activities in rat and human brain. *Neurochem. Int.* **40,** 337–345
57. Venäläinen, J. I., Garcia-Horsman, J. A., Forsberg, M. M., Jalkanen, A., Wallén, E. A. A., Jarho, E. M., Christiaans, J. A., Gynther, J., and Männistö, P. T. (2006) Binding kinetics and duration of *in vivo* action of novel prolyl oligopeptidase inhibitors. *Biochem. Pharmacol.* **71,** 683–692
58. Younis, A. E., Soblik, H., Ajonina-Ekoti, I., Erttmann, K. D., Luersen, K., Liebau, E., and Brattig, N. W. (2011) Characterization of a secreted macrophage migration inhibitory factor homologue of the parasitic nematode *Strongyloides* acting at the parasite-host cell interface. *Microbes Infect.* Oct 17. [Epub ahead of print]
59. Mimori, T., Tanaka, M., and Tada, I. (1987) *Strongyloides ratti:* Formation of protection in rats by excretory/secretory products of adult worms. *Exp. Parasitol.*, **64,** 342–346
60. Eschbach, M. L., Klemm, U., Kolbaum, J., Blankenhaus, B., Brattig, N., and Breloer, M. (2010) *Strongyloides ratti* infection induces transient nematode-specific Th2 response and reciprocal suppression of IFN-gamma production in mice. *Parasite Immunol.* **32,** 370–383
61. Hewitson, J. P., Harcus, Y. M., Curwen, R. S., Dowle, A. A., Atmadja, A. K., Ashton, P. D., Wilson, A., and Maizels, R. M. (2008) The secretome of the filarial parasite, *Brugia malayi*: proteomic profile of adult excretory-secretory products. *Mol. Biochem. Parasitol.* **160,** 8–21
62. Mulvenna, J., Hamilton, B., Nagaraj, S. H., Smyth, D., Loukas, A., and Gorman, J. J. (2009) Proteomics analysis of the excretory/secretory component of the blood-feeding stage of the hookworm, *Ancylostoma caninum. Mol. Cell. Proteomics.* **8,** 109–121
63. Robinson, M. W., Menon, R., Donnelly, S. M., Dalton, J. P., and Ranganathan, S. (2009) An integrated transcriptomics and proteomics analysis of the secretome of the helminth pathogen *Fasciola hepatica*: proteins associated with invasion and infection of the mammalian host. *Mol. Cell. Proteomics.* **8,** 1891–1907
64. Knudsen, G. M., Medzihradszky, K. F., Lim, K. C., Hansell, E., and McKerrow, J. H. (2005) Proteomic analysis of *Schistosoma mansoni* cercarial secretions. *Mol. Cell. Proteomics* **4,** 1862–1875
65. Hartmann, S., Sereda, M. J., Sollwedel, A., Kalinna, B., and Lucius, R. (2006) A nematode allergen elicits protection against challenge infection under specific conditions. *Vaccine* **24,** 3581–3590
66. Sereda, M. J., Hartmann, S., Büttner, D. W., Volkmer, R., Hovestädt, M., Brattig, N., and Lucius, R. (2010) Characterization of the allergen filarial tropomyosin with an invertebrate specific monoclonal antibody. *Acta Trop.* **116,** 61–67
67. Johnston, M. J., MacDonald, J. A., and McKay, D. M. (2009) Parasitic helminths: a pharmacopeia of anti-inflammatory molecules. *Parasitology* **136,** 125–147